
[All ETDs from UAB](#)

[UAB Theses & Dissertations](#)

2019

Design Of A Truck-Mounted Attenuator With Tube Folding Technology

Santosh Gautam
University of Alabama at Birmingham

Follow this and additional works at: <https://digitalcommons.library.uab.edu/etd-collection>



Part of the [Engineering Commons](#)

Recommended Citation

Gautam, Santosh, "Design Of A Truck-Mounted Attenuator With Tube Folding Technology" (2019). *All ETDs from UAB*. 1718.

<https://digitalcommons.library.uab.edu/etd-collection/1718>

This content has been accepted for inclusion by an authorized administrator of the UAB Digital Commons, and is provided as a free open access item. All inquiries regarding this item or the UAB Digital Commons should be directed to the [UAB Libraries Office of Scholarly Communication](#).

DESIGN OF A TRUCK-MOUNTED ATTENUATOR WITH TUBE FOLDING
TECHNOLOGY

by

SANTOSH GAUTAM

DEAN SICKING, COMMITTEE CHAIR

DAVID LITTLEFIELD

LEE MORADI

A THESIS

Submitted to the graduate faculty of The University of Alabama at Birmingham,

in partial fulfillment of the requirements for the degree of

Master of Science

BIRMINGHAM, ALABAMA

2019

DESIGN OF A TRUCK-MOUNTED ATTENUATOR WITH TUBE FOLDING TECHNOLOGY

SANTOSH GAUTAM

MECHANICAL ENGINEERING

ABSTRACT

Highway safety features have been continuously developed and employed over the years to protect vehicle occupants, pedestrians and work zone personnel from injuries in roadside accidents. The new truck-mounted attenuator designed and evaluated in this study aims to dissipate impacting energy of the errant vehicle in a controlled manner using a tube folding mechanism. Finite element modeling using LS-DYNA is used to study the performance of the designed truck-mounted attenuator. It is required to safely bring passenger vehicles travelling at a speed of 62 mph to a stop by keeping the occupant safety criteria within limits recommended by the Manual for Assessing Safety Hardware (MASH). Several finite element models have been developed to simulate impact with a small car and a pickup truck. The optimized finite element model is found to dissipate the impacting energy of the colliding vehicle by satisfying the occupant safety criteria. Experimental tests are required to validate the numerical models. Future research can be built upon findings of this study for further developments.

ACKNOWLEDEGEMENT

I wish to express my gratitude to Dr. Dean Sicking, my thesis advisor for his continuous guidance, support and encouragement throughout my research study. I would also like to thank Dr. David Littlefield and Dr. Lee Moradi, the members of my thesis committee for their time and support.

I would like to express my sincere gratitude to Dr. Kent Walls and Dr. Kevin Schrum for their time, guidance and suggestions throughout this study. I would also like to thank Sherrye Watson in UAB Mechanical Engineering for her help during my graduate degree.

Finally, I would like to thank my family and friends for their continuous love, encouragement and support in my life.

TABLE OF CONTENTS

ABSTRACT.....	ii
ACKNOWLEDEEMENT.....	iii
LIST OF FIGURES	vi
LIST OF TABLES	ix
CHAPTER 1- INTRODUCTION.....	1
1.1. Background	1
1.2. Problem Statement	2
1.3. Objective of the Research	4
CHAPTER 2- LITERATURE REVIEW AND DESIGN CRITERIA.....	6
2.1. Previous Research	6
2.2. Design Criteria	8
2.3. Occupant Risk	11
2.3.1. <i>Occupant Flail-Space Model</i>	11
2.3.2. <i>Occupant Impact Velocity (OIV)</i>	12
2.3.3 <i>Ride-Down Acceleration (RA)</i>	15
CHAPTER 3- DESIGN	17
3.1. Analytical Model.....	17
3.1.1 <i>Analytical Results</i>	19
3.2. TMA Design.....	22

3.3. Numerical Model.....	26
3.3.1 <i>Material Model</i>	26
CHAPTER 4- FINITE ELEMENT MODELING	29
4.1. Basic Finite Element Model.....	29
4.2. Progression of Finite Element Models	33
4.2.1 <i>Mesh Resolution Study</i>	33
4.2.2. <i>Parametric Study on Tube Wall Thickness</i>	35
4.2.3. <i>Model 1</i>	40
4.2.4. <i>Model 2</i>	43
4.2.5. <i>Model 3</i>	47
4.2.6. <i>Model 4</i>	50
4.2.7. <i>Effect of Outlet Pipes</i>	52
4.2.8. <i>Effect of Mass of the Impact Head</i>	54
CHAPTER 5- RESULTS AND DISCUSSION	58
5.1. Sequential Images	58
5.2. Results for Test 3-50	64
5.3. Results for Test 3-51	67
5.3. Occupant Safety Parameters.....	71
CHAPTER 6- CONCLUSIONS AND RECOMMENDATIONS.....	74
6.1. Conclusions	74
6.2. Recommendations	75
REFERENCES	76

LIST OF FIGURES

Figure 1.1. TMA employed in work zone.....	2
Figure 2.1. Velocity-time diagram of crashing vehicle with unrestrained occupant.	13
Figure 2.2. Velocity-time diagram of crashing vehicle with restrained occupant.	14
Figure 3.1. 3-D model of the designed TMA.....	23
Figure 3.2. Squeezer tube with wedges welded horizontally.....	24
Figure 3.3. 3-D models showing front and back views of the impact head.....	25
Figure 3.4. Elastic-plastic behavior with isotropic and kinematic hardening.....	27
Figure 4.1. Basic finite element model of the tube folding mechanism.	30
Figure 4.2. Force produced by the tube with wall thicknesses 12 gauge and 10 gauge. ..	32
Figure 4.3. Force produced by the tube with wall thicknesses 10 gauge and 7 gauge.	32
Figure 4.4. Forces produced by the tube for various mesh sizes	34
Figure 4.5. Three-tube model developed for study of the effect of tube wall thickness. .	35
Figure 4.6. Force produced by tubes with various wall thicknesses.....	36
Figure 4.7. Velocity of the impacting rigid plate for different tube thicknesses.	37
Figure 4.8. Plots of displacement for the impacting rigid plate with different tube thicknesses.	38
Figure 4.9. Kinetic energy of the rigid plate for tubes of various wall thicknesses.....	39
Figure 4.10. Three-tube model with a rigid plate simulated as the vehicle.	41

Figure 4.11. Accelerations from test 3-50 in Model 1.....	42
Figure 4.12. Accelerations from test 3-51 in Model 1.....	42
Figure 4.13. Finite element model simulating test 3-50 for the small car.	44
Figure 4.14. Finite element model simulating test 3-51 for the pickup truck.....	44
Figure 4.15. Longitudinal ride-down accelerations for tests 3-50 and 3-51.	45
Figure 4.16. Test 3-50 showing the possibility of the TMA running over the car.	46
Figure 4.17. Model 3 with four wall thicknesses along the length of the tubes.	48
Figure 4.18. Longitudinal vehicular acceleration for test 3-50.....	49
Figure 4.19. Longitudinal vehicular acceleration for test 3-51.....	49
Figure 4.20. Final finite element model of the TMA consisting of tubes with three different wall thicknesses.....	51
Figure 4.21. Kinetic energy of the pickup truck for study of effects of outlet pipes.....	53
Figure 4.22. Effect of mass of impact head on vehicular accelerations.	56
Figure 4.23. Effect of mass of impact head on vehicular velocities.	56
Figure 5.1. Sequential images of test 3-50.....	60
Figure 5.2. Sequential images of test 3-51.....	61
Figure 5.3. Sequential images of test 3-52.....	62
Figure 5.4. Sequential images of test 3-53.....	63
Figure 5.5. Accelerations in the small car model for different coefficients of friction. ...	64
Figure 5.6. Velocity plots for the car model for different friction coefficients.	65
Figure 5.7. Displacement of the car with time for different coefficients of friction.....	65
Figure 5.8. Energy balance for test 3-50.....	67
Figure 5.9. Acceleration plots for the pickup truck for different friction coefficients.	68

Figure 5.10. Velocity plots of the pickup truck model for different friction coefficients.	68
Figure 5.11. Displacement of the pickup truck with time for different friction coefficients.	69
Figure 5.12. Kinetic energy of the pickup truck for different friction coefficients.	70
Figure 5.13. Energy balance for test 3-51.....	71

LIST OF TABLES

Table 2.1. Test levels defined by MASH.....	8
Table 2.2. Test matrices for truck-mounted attenuators recommended by MASH.	9
Table 2.3. OIV limits for TMAs recommended by MASH.....	15
Table 2.4. RA values for TMAs recommended by MASH.	16
Table 3.1. Analytical model for 2425 lb car.	21
Table 3.2. Analytical model for 5004 lb pickup truck.....	21
Table 3.3. Properties of material used in the finite element models.....	28
Table 4.1. Forces produced in the models with different tube thicknesses.	33
Table 4.2. Average force produced by tubes with different wall thicknesses.	36
Table 4.3. Kinetic energy of the rigid plate dissipated by tubes with different wall thicknesses.	39
Table 4.4. Occupant ride-down acceleration (RA) values for Model 1.....	43
Table 4.5. Longitudinal OIVs for tests 3-50 and 3-51 for Model 2.....	46
Table 4.6. Longitudinal occupant ride-down accelerations in Model 3.	50
Table 4.7. Longitudinal occupant impact velocities in Model 3.....	50
Table 4.8. Effect of outlet pipes in energy dissipation.	54
Table 4.9. Mass of different impact heads considered.....	55
Table 4.10. Longitudinal occupant RA for models with different impact heads.....	57

Table 5.1. Average forces produced in the model for test 3-50.....	66
Table 5.2. Average forces produced in the model for test 3-51.....	70
Table 5.3. Occupant risk factors from finite element models for tests 3-50 to 3-53.	73

CHAPTER 1- INTRODUCTION

1.1. Background

Several highway safety features (devices) have been developed and employed over the years to prevent/ reduce the number of injuries and fatalities. Longitudinal barriers, terminals, crash cushions, support structures, work-zone attenuation and channelizers, traffic gates, arrestors, and drainage and geometric features are some of the permanent and temporary highway safety features. The goal of a highway safety feature is to provide a forgiving roadway and roadside that reduces the risk of a serious accident when a motorist leaves the roadway. The functions of various safety features vary between containing and redirecting a vehicle away from a roadside obstacle, decelerating the vehicle to a safe stop, readily breaking away or yielding, allowing a controlled penetration, and acting traversable. The purpose of each of these functions is to prevent serious injuries to the occupants of the vehicle, other motorists, pedestrians and work zone personnel (AASHTO, 2009).

A truck mounted attenuator (TMA) is a mechanical structure that is mounted on the rear side of a work zone vehicle, used to block errant vehicles from entering the work zone. When an errant vehicle leaves the roadway and tries to intrude into the work zone, the support truck which houses the TMA is placed strategically so that the TMA acts as an

attenuation device to bring the vehicle to a controlled stop. TMAs are usually utilized in roadway maintenance, repair and construction applications. A TMA basically consists of two components: (1) an energy absorber and (2) a docking station (platform). The energy absorber rests on the platform and is foldable when not in use. Figure 1.1 depicts an example of a commercially available TMA.

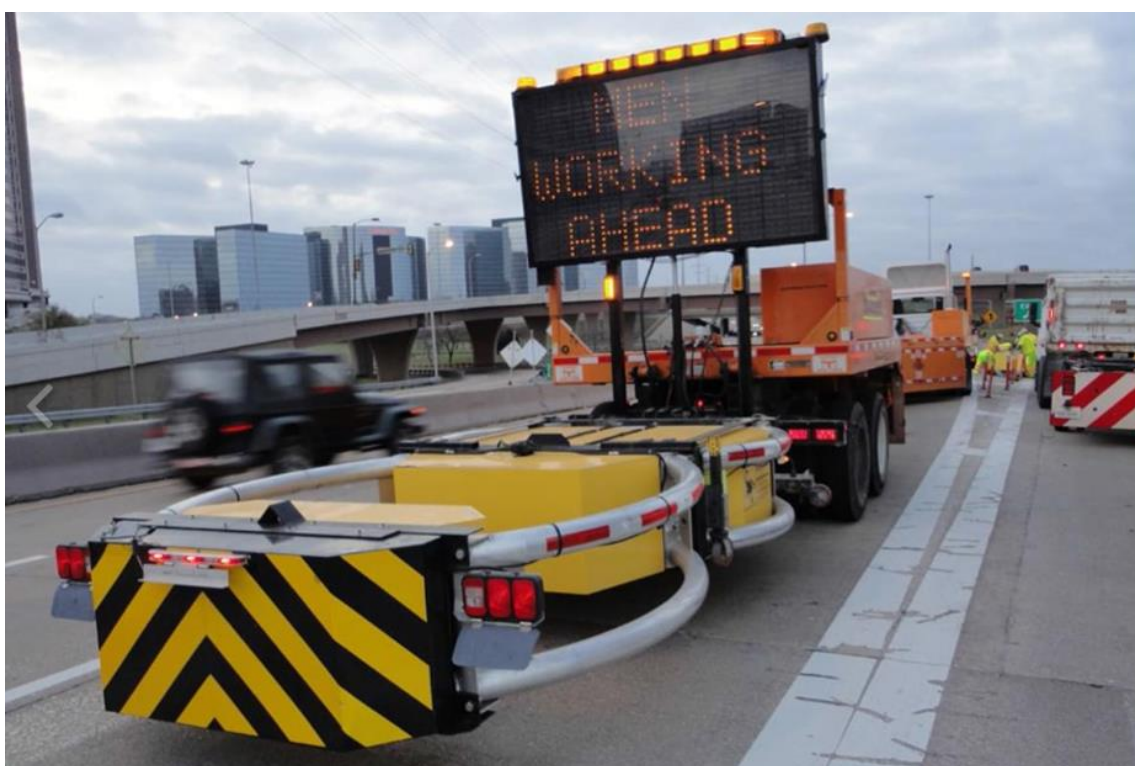


Figure 1.1. TMA employed in work zone.

(<https://www.traffixdevices.com/products/attenuators/scorpion2-tma>)

1.2. Problem Statement

A large number of road accidents occur every year in the United States and around the world. According to the National Highway Traffic Safety Administration (NHTSA),

about 6.45 million crashes occurred in 2017 in the USA claiming the lives of 37,133 people and injuring 2.75 million people. The fatality rate per 100 million vehicle miles travelled was 1.16, and the injury rate per 100 million vehicle miles travelled was 85 (National Highway Traffic Safety Administration, 2017). According to the Global Status Report on Road Safety 2018 by the World Health Organization (WHO), about 1.35 million people die globally due to road traffic accidents. Road traffic injuries are the 8th leading cause of death for people of all ages in the world (World Health Organization, 2018).

Truck-mounted attenuators (TMAs) act to decelerate an errant vehicle to a safe stop when it leaves the roadway and enters a work zone. The support trucks usually have high mass compared to an errant passenger vehicle. So, the occupant(s) inside the errant vehicle are injury-prone if the TMA does not provide controlled energy dissipation of the impacting vehicle. However, if the mass of the support truck is small, it may also cause injuries to the driver of the support truck and other work zone personnel due to movement of the support truck.

Design of the energy absorber of the TMA needs to be concise from material, cost and safety perspectives without compromising energy absorption efficiency of the mechanism. The Manual for Assessing Safety Hardware (MASH) provides uniform guidelines for crash testing and recommends evaluation criteria to assess test results for a majority of highway safety features. Three major dynamic evaluation factors mandated by MASH are: (1) structural adequacy, (2) occupant risk, and (3) post-impact vehicular response (AASHTO, 2009). The occupant risk criteria for design of a TMA is concerned with occupant impact velocity (OIV) and occupant ride-down acceleration (ORA) values as recommended by MASH. The TMA should have structural adequacy and energy

absorption efficiency to stop an errant vehicle intruding into a work zone by limiting the occupant impact velocity and ride-down accelerations within the recommended values.

1.3. Objective of the Research

The major objective of the research is to design and develop a truck mounted attenuator which utilizes a novel tube folding energy absorption mechanism. TMAs are costly and can be difficult to install. The goal of the new TMA design is to provide an economical alternative to existing systems. This study will require development of a new energy absorption system and will use computational mechanics to evaluate the design.

The design of a highway safety feature requires application of principles of mechanics to develop an analytical model. Static tests, dynamic tests and computer simulations are used to evaluate impact performance of the safety feature under different test conditions, and to conduct parametric studies. The design is modified based on the results of experimental and computational studies. Full-scale crash tests are the most definitive way to evaluate a highway safety feature. However, these tests are expensive and are not feasible to be repeated for all candidate designs. Computational tools have proven to be reliable and cost-effective methods of development and testing of candidate safety features. Finite element analysis codes such as LS-DYNA have proven to be strong analysis tools and have been widely used by researchers around the world for design and development of highway safety features. Despite the recent development in computational tools and their increased accuracy, full scale crash testing is not replaceable and is used as a guideline to validate computational models. Computational models when verified by full-

scale crash testing can be very effective, cost-effective and faster methods of design and development of highway safety features.

The specific objectives of this research study are as follows:

- a) Study of available literature to identify criteria for design, testing and evaluation of highway safety features.
- b) Study of available literature on the design and testing of truck- and trailer-mounted attenuators.
- c) Design of a TMA with novel tube folding energy absorber. Address test guidelines and evaluation criteria defined in MASH.
- d) Perform computational study via development of LS-DYNA models for all candidate TMA designs. Develop computational models for different test conditions. Perform parametric study. Identify the design that best addresses evaluation criteria defined by MASH.
- e) Provide conclusions and recommendations for future research study.

CHAPTER 2- LITERATURE REVIEW AND DESIGN CRITERIA

2.1. Previous Research

There have been some studies in the past that have utilized several energy absorption mechanisms for the development of crash cushions, truck-mounted attenuators and trailer-mounted attenuators. Sicking et al. successfully developed and crash-tested the design of a trailer-attenuating cushion for arrow boards and variable message signs with the use of a tube-bursting energy absorption mechanism. In the design, tapered mandrels were forced into steel tubes, and initiation and propagation of cracks along the length of the tubes was controlled to dissipate energy of an impacting vehicle. Sicking et al. through the utilization of LS-DYNA modeling and dynamic testing, found that factors having the greatest influence on energy dissipation were size and thickness of the bursting tubes as well as friction between the mandrels and the tubes. The design also utilized an impact head that functioned to produce a mechanical interlock with the frontal face of the impacting vehicle in order to control the loads between the attenuating cushion and the impacting vehicle (Dean L. Sicking, 2003).

Waszczuk in his study developed a finite element model of a truck-mounted attenuator using ABAQUS Unified FEA, aided by static testing and impact testing. He utilized multiple cells made of aluminum sheet to develop prototypes for field testing using a bogie vehicle. Waszczuk in his work successfully demonstrated a close resemblance of

results from finite element models with results from static and impact tests (Waszczuk, 2013). Belingardi and Obradovic in their research paper developed numerical models to design an impact attenuator for a Formula SAE student race car for frontal body safety. Finite element models were developed in Hyper Mesh to optimize the design of the attenuator for maximum energy dissipation. With attachment of the attenuator to car body frame, the paper concluded to have limited the average deceleration of the car post impact to within 20 g's as mandated by SAE rules (Giovanni Belingardi, 2010).

Buyuk et al. developed and crash tested a crash cushion made of polyethylene containers, for application in roads with 50 kph (31 mph) speed limits. They developed finite element models with LS-DYNA and performed full-scale crash testing to validate the FE models. Impact performance of the crash cushion at higher speeds was not addressed by the study (Murat Buyuk, 2018). Carney et al. in their research study also developed a reusable crash cushion made of polyethylene thermoplastic. They utilized finite element models created using DYNA3D software to model impacts using varieties of test conditions and carried out full-scale crash tests to validate the reusability of the crash cushion (John F. Carney, 1999).

A limited number of published literatures are available involving the design and testing of truck-mounted attenuators. However, available literature on crash cushions and different types of impact attenuators mentioned above can be used as references for understanding finite element modeling, impact testing and application of work-zone attenuation devices. There are some commercially available truck-mounted attenuators but there are no literary publications concerning these products.

2.2. Design Criteria

The design of roadside safety features is bound by the guidelines for crash testing and evaluation criteria defined by the Manual for Assessing Safety Hardware (MASH). Published in 2009 by the American Association of State Highway and Transportation Officials (AASHTO), MASH is an update to and supersedes the National Cooperative Highway Research Program (NCHRP) Report 350. MASH has defined test levels for all temporary and permanent roadside safety features. A truck-mounted attenuator (TMA) can be subjected to one of the three test levels. Each test level is defined by impact conditions (speed and angle of approach of the impacting vehicle) and the type of the testing vehicle (AASHTO, 2009). Table 2.1 shows test levels 1, 2 and 3 defined by MASH which are relevant to TMAs.

Table 2.1. Test levels defined by MASH.

Test Level	Test Vehicle Designation and Type	Test Conditions	
		Speed mph (ft/s)	Maximum Angle (deg)
1	1100C (passenger car)	31 (45.47)	25
	2270P (pickup truck)	31 (45.47)	25
2	1100C (passenger car)	44 (64.53)	25
	2270P (pickup truck)	44 (64.53)	25
3	1100C (passenger car)	62 (90.93)	25
	2270P (pickup truck)	62 (90.93)	25

A roadside safety feature designed and tested for a low-test level is to be used on a low-speed and/or low-volume roadway, whereas that designed and tested for a high-test level is to be used on a high-speed and/or high-volume roadway. The TMA designed in this research study is targeted to be used in the work-zone on freeways. So, test level 3 applies to the newly designed TMA i.e. it should be capable of dissipating impact energy of a passenger car weighing 1100 kg (2425 lb) and a light pickup truck weighing 2270 kg (5004 lb) both travelling at a speed of 62 mph (90.93 ft/s). The impact conditions outlined in Table 2.1 represent the worst practical condition for a roadside feature crash (AASHTO, 2009).

MASH recommends tests 50, 51, 52 and 53 for truck-mounted attenuators. Tests 50, 51 and 52 should be conducted with the heaviest allowable support truck (or rigidly blocked support truck for unlimited weight) while test 53 should be conducted with the lightest allowable support truck. A rigidly blocked support vehicle has been assumed in this study for all tests. Table 2.2 shows recommended test matrices for TMAs.

Table 2.2. Test matrices for truck-mounted attenuators recommended by MASH.

Test Level	Test No.	Test Vehicle	Impact speed (mph)	Impact angle (deg.)
3	3-50	1100C	62	0
	3-51	2270P	62	0
	3-52	2270P	62	0
	3-53	2270P	62	10

Test 3-52 consists of an offset impact with the pickup truck where the offset distance from centerline of the TMA to the centerline of the pickup truck is one-third of the width of the pickup truck, i.e. one-third of 78 in = 26 in. Test 3-53 consists of an angular-offset impact where the angle between the centerline of the TMA and the centerline of the pickup truck is 10 degrees, with an offset distance of one-fourth of the width of the truck, i.e. 19.5 inches.

There are three major evaluation criteria used to evaluate the impact performance of roadside safety features- a) structural adequacy, b) occupant risk and c) post-impact vehicular response. Structural adequacy requires a safety feature to satisfactorily perform the intended functions of the feature. TMAs are required to provide controlled stopping of the impacting vehicle. The ideal impact energy absorption involves a constant resisting force with time by the structural elements of the TMA so that instantaneous peaks are avoided. However, in practical conditions, the resisting forces from TMA to the impacting vehicle will have peaks at certain intervals (usually during impact), and there is always some noise due to different factors such as vibration, non-uniformity in energy absorbing material, etc. Post-impact vehicular response criteria require the impacting vehicle and the test article (TMA with support truck) to have minimum chances of obstructing or colliding with other vehicles, and injuring pedestrians, occupants of other vehicles and work-zone personnel (AASHTO, 2009). Since TMAs are designed to mostly absorb end-on impacts and bring errant vehicles to a controlled slowdown or stop, the likelihood of the impacting vehicle directing away from the initial travel path should be minimized. Also, the minimum weight of the support truck should be fixed to avoid excessive movement of the support truck which could cause injury to the support truck driver and other work-zone personnel.

These issues are taken into consideration by designing an impact head that provides a mechanical interlock with the frontal face of the impacting vehicle as well as using support trucks that have very high mass compared to the mass of the impacting passenger car and pickup truck. Occupant risk will be discussed in detail in the following segment.

2.3. Occupant Risk

Occupant risk is the most important criteria while designing and installing roadway safety features. The risk of injury to occupants of the impacting vehicle during collision with roadside safety features depends to a great extent on the crashworthiness of the impacting vehicle. Since crashworthiness varies greatly for a wide range of vehicles, occupant safety is analyzed in terms of vehicular accelerations developed during the course of impact. Two important factors are considered to measure occupant risk- occupant impact velocity (OIV) and ride-down acceleration (RA) (AASHTO, 2009). These factors are defined based on the occupant flail-space model.

2.3.1. Occupant Flail-Space Model

Occupant risk is assessed based on the motion of an unrestrained front seat occupant in the event of an impact. The collision consists of two phases. In phase 1, the unrestrained occupant is displaced through the vehicle compartment (flail space) until he/she strikes the instrument panel, wind shield or side door with injury-dependent velocity. In phase 2 of the impact, the occupant experiences vehicular accelerations perpendicular to the contact

surface by remaining in contact with it (rides down with the vehicle) and is subjected to injury-dependent accelerations (Mitchie).

The distance travelled by the occupant relative to the vehicle before contact with the vehicle interior is assumed to be 24 inches (2 ft) in the longitudinal direction of vehicle travel (distance to instrument panel) and 12 inches (1 ft) in the lateral direction (distance to side door). Restraint systems such as seat belts, air bags, collapsible steering columns, knee bolsters, etc. are found in modern vehicles, which increase the time taken by the occupant to come in contact with the vehicle interior. For occupant risk assessment, these restraint systems are assumed to be absent in the vehicle (Mitchie).

2.3.2. Occupant Impact Velocity (OIV)

Bois et al. in their book have explained occupant response through velocity-time diagrams for restrained and unrestrained occupant cases. Figure 2.1 shows a velocity-time diagram for a vehicle crashing with a rigid barrier, with an unrestrained occupant. It takes into consideration a vehicle speed of 30 mph (48 kph), 24 inches of vehicle frontal crush, and 24 inches between the occupant and instrument panel. It can be seen from the velocity-time diagram that the unrestrained occupant after contact with the panel will experience rapid deceleration (Paul Du Bois, 2004).

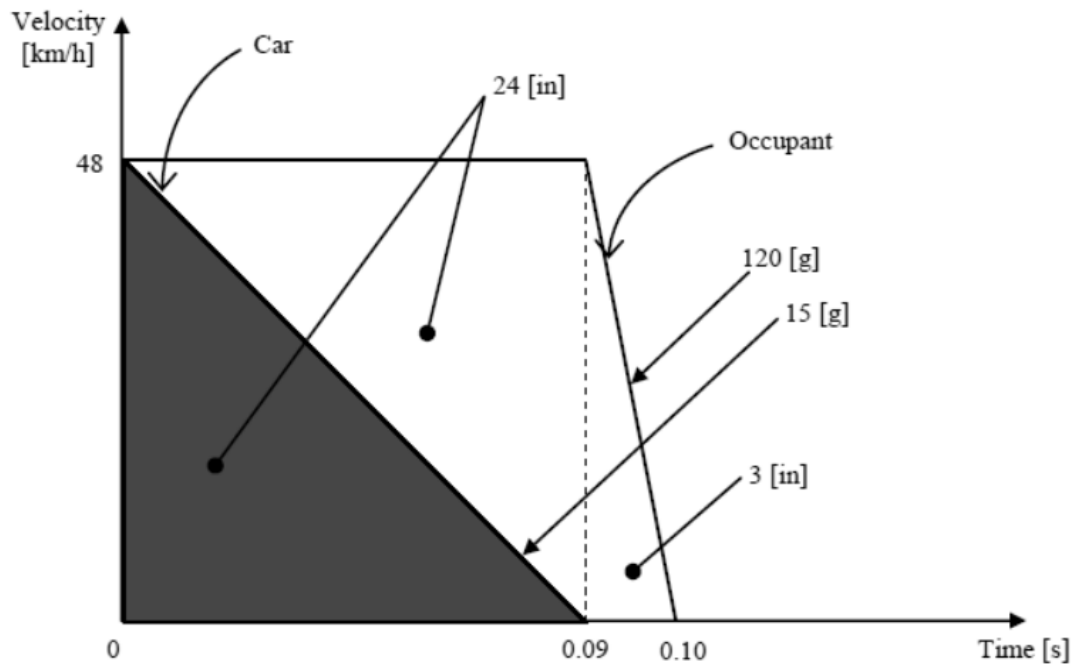


Figure 2.1. Velocity-time diagram of crashing vehicle with unrestrained occupant.

(Paul Du Bois, 2004)

Figure 2.2 shows a velocity-time diagram of the crashing vehicle with a restrained occupant. Due to some slack in the restraint system, there is an initial relative displacement between the occupant and the vehicle. The restraint system then acts to bring the occupant to rest. Depending upon whether the occupant comes to rest together with the vehicle or after the vehicle is stopped, different accelerations act on the occupant. It can be noticed easily that due to action of the restraint system, the deceleration forces acting on the occupant are significantly reduced.

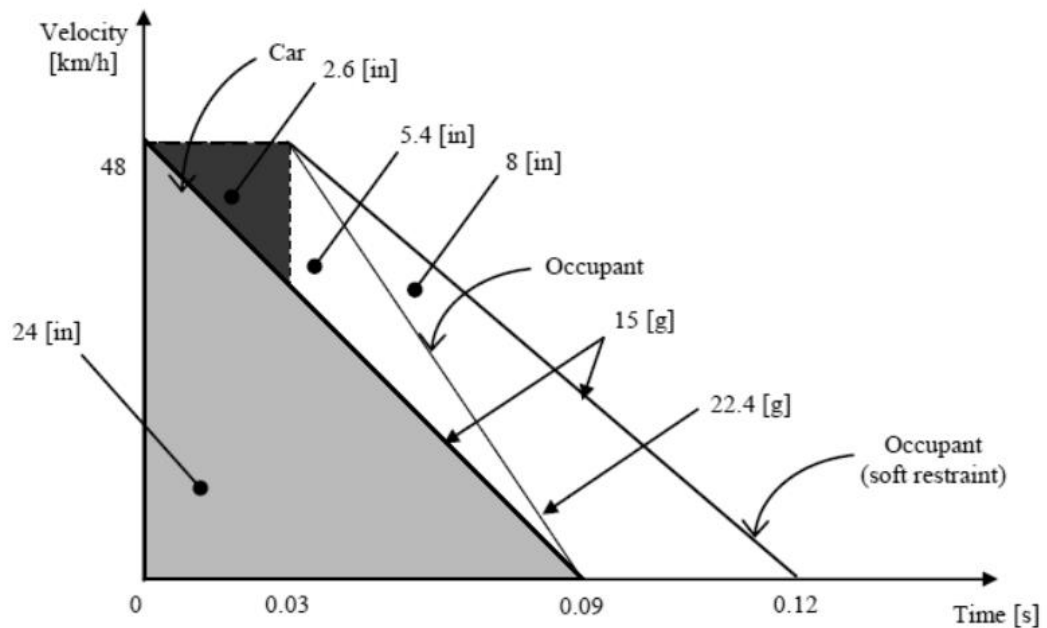


Figure 2.2. Velocity-time diagram of crashing vehicle with restrained occupant.

(Paul Du Bois, 2004)

The diagrams described above consider a rigid barrier, so the unrestrained occupant strikes the vehicle interior with the initial velocity of the vehicle. All roadside safety features have energy dissipation properties. However, the challenge is to gradually dissipate energy of the impacting vehicle so that the relative velocity of the occupant with respect to the vehicle is low when the occupant strikes the vehicle interior. Upon impact, the unrestrained occupant continues moving forward (or sideways) with the pre-impact velocity while the impacting vehicle slows down gradually depending upon the energy dissipation characteristics of the roadway safety feature. The occupant strikes the vehicle interior with a velocity that is relative to the velocity of the vehicle. This relative velocity is called the occupant impact velocity (OIV). The OIV is critical in the design of roadway

safety features and treatment systems because it is directly responsible for causing injuries to the occupants.

The safety feature evaluation guidelines in MASH require the lateral and longitudinal components of occupant impact velocity (OIV) within limits that will minimize the risk of injury to the occupants. Table 2.3 below lists the OIV limits recommended by MASH applicable for truck-mounted attenuators (tests 3-50, 3-51, 3-52 and 3-53).

Table 2.3. OIV limits for TMAs recommended by MASH.

Occupant impact velocity limits, ft/s (m/s)		
Component	Preferred	Maximum
Longitudinal and lateral	30ft/s (9.1 m/s)	40 ft/s (12.2 m/s)

2.3.3 Ride-Down Acceleration (RA)

After an unrestrained occupant comes in contact with the interior component of the vehicle during impact, the occupant rides down with the vehicle and experiences vehicular accelerations perpendicular to the contact surface. Since there is dissipation of energy of the impacting vehicle due to action of the roadway safety feature, negative acceleration (deceleration) acts on the occupant. For ideal energy dissipation without the presence of peaks, the force experienced by an occupant throughout the impact is given by $F = ma$, where m is the mass of the occupant and a is the deceleration of the vehicle (along with the occupant). In practical conditions, the forces vary with time due to noise. High values of

decelerations can cause severe injuries to the occupant. Some examples of levels of acceleration found in the real world are listed below (Waszczuk, 2013).

- A roller coaster can produce maximum accelerations of 3 to 4 g's.
- Accelerations during the crash of Princess Diana of Wales in 1997 was in the range of 70 to 100 g's.
- Blackouts or death can occur if an acceleration of 4 to 6 g's is maintained for more than few seconds.

Roadside safety feature evaluation guidelines in MASH require monitoring of the highest lateral and longitudinal components of vehicular acceleration averaged over 10-ms interval for the collision pulse after occupant impact occurs (AASHTO, 2009). Table 2.4 below lists the ride-down acceleration (RA) limits recommended by MASH applicable to TMAs (tests 3-50, 3-51, 3-52 and 3-53).

Table 2.4. RA values for TMAs recommended by MASH.

Occupant ride-down acceleration limits (g)		
Component	Preferred	Maximum
Longitudinal and lateral	15 g	20.49 g

The decelerations (and forces) acting on the occupant depend on the energy dissipation characteristics of the highway safety feature. In case of TMAs, sufficient travel for the impacting vehicle after impact with the TMA is required to control the forces acting on the occupant. The size of a TMA is desired to be compact and cost-effective for practical purposes. This poses challenges to the designers of TMAs and other attenuation devices.

CHAPTER 3- DESIGN

3.1. Analytical Model

The design of a truck mounted attenuator involves energy dissipation by converting kinetic energy of the impacting vehicle primarily to the work done during plastic deformation of components of the TMA. A portion of the kinetic energy of the vehicle is also dissipated in overcoming inertial and frictional energies. In the design proposed in this research study, energy is dissipated by plastic deformation (folding) of steel tubes when they pass through components called squeezers. The principle of conservation of linear momentum and the principle of conservation of energy govern the energy dissipation process- kinetic energy of the impacting vehicle lost during the impact is converted to work done by the vehicle in deforming the steel tubes.

The linear momentum of a vehicle of mass m travelling at a velocity \vec{v} is given by:

$$\vec{p} = m \times \vec{v} \quad (3.1)$$

The force applied to or by an object is equal to the rate of change of linear momentum of the object.

$$\vec{F} = \frac{d\vec{p}}{dt} \quad (3.2)$$

The differential work produced by this force over an infinitesimally small displacement $d\vec{s}$ is given by

$$dW = \vec{F} \cdot d\vec{s} \quad (3.3)$$

where $d\vec{s}$ is the infinitesimally small displacement over time dt .

The net work done by the force over the displacement s is given by the integral:

$$W = \int_0^s \vec{F} \cdot d\vec{s} \quad (3.4)$$

If a vehicle of mass m having velocity \vec{v}_1 undergoes a change in velocity such that its velocity after time t becomes \vec{v}_2 , the work done by the vehicle or work done on the vehicle is equal to the difference between the final and initial kinetic energies of the vehicle.

$$W = \Delta K.E. = \frac{m(v_2^2 - v_1^2)}{2} \quad (3.5)$$

Kinetic energy and momentum of an object at a certain instant of time can be related as:

$$K.E. = p \times \frac{v}{2} \quad (3.6)$$

When an errant vehicle impacts the TMA, it loses kinetic energy gradually and produces work by plastic deformation of the structural elements of the TMA. This can be seen from equation 3.5 where if the final velocity of an object is less than the initial velocity, the work done is negative. Also, it can be seen that if an errant vehicle is brought to a complete stop, the total work done by the vehicle is equal to its entire initial kinetic energy, i.e. the TMA has to dissipate all of the pre-impact kinetic energy the vehicle possessed. Equation 3.5 also assumes that the TMA has a rigid immovable support i.e. the weight of the support truck is very high compared to the impacting vehicle and there is no movement of the support truck during impact. In real world crashes, there is some movement in the support truck during impact, so that a portion of the initial kinetic energy of the impacting vehicle is converted to the kinetic energy of the support truck.

3.1.1 Analytical Results

The basic idea involved with this TMA design is to deform a steel tube by forcing it inside a squeezer that systematically deforms and collapses the tube to absorb energy of the impacting vehicle. Details on the design features of the TMA are explained in subsequent sections. The impact head and tubes assembly have a mass of about 310 kg (683 lbs). This stationary mass acts as an additional source of energy dissipation when the vehicle strikes the TMA. After the initial impact, the vehicle and assembly of the impact head and tubes move at the same speed throughout the remainder of the impact.

Analytical models are developed for tests 3-50 and 3-51 involving the small car (2425 lb) and the pickup truck (5004 lb) respectively. For the purpose of this analysis, for test 3-50, OIV is assumed to be 40 ft/s and RA is assumed to be a constant value of 18 g's. For test 3-51, OIV is assumed to be 35ft/s and RA is assumed to be a constant value of 15 g's. These values are within the limits recommended by MASH. Analytical models for tests 3-50 and 3-51 are shown in Tables 3.1 and 3.2.

From Table 3.1, it can be seen that the initial kinetic energy of the car travelling at 91.67 ft/s (62.5 mph) is 317 kip-ft. After collision with the impact head, the speed of the car is reduced to 71.51 ft/s (48.76 mph) due to momentum transfer to the stationary assembly of the impact head and folding tubes. The calculation of values in Table 3.1 is shown below.

When the car impacts with the stationary mass of the TMA, from the principle of conservation of linear momentum, $m_1 \times v_1 = m_2 \times v_2$.

$$\text{i.e. } 1100 \times 91.67 = (1100 + 310) \times v_2$$

$$\therefore v_2 = 71.51 \text{ ft/s}$$

which is the speed at which the car and the stationary mass move ahead.

At the instant when occupant impact occurs, the speed of the car is the difference in the initial speed of the car and the value of OIV.

$$\text{i.e. speed of the car} = 91.67 - 40 = 51.67 \text{ ft/s}$$

The displacement of the car until the time when OIV occurs is calculated by using the equation of motion, $v^2 = u^2 + 2as$

$$\text{where, } v = \text{final speed of the car} = 51.66 \text{ ft/s}$$

$$u = \text{initial speed of the car} = 71.51 \text{ ft/s}$$

$$a = \text{acceleration of the car} = -18 \text{ g} = -579 \text{ ft/s}^2$$

$$\therefore \text{Distance travelled by the car (s)} = 2.11 \text{ ft}$$

The distance travelled by the car after the instant of occupant impact to stop is also calculated using the same concept.

Table 3.1. Analytical model for 2425 lb car.

Instances	Speed of the car, ft/s (mph)	K.E. of the car (kip-ft)	ΔK.E. (kip-ft)	Displacement (ft)
Pre-impact	91.67 (62.5)	316.54	-	-
Impact with stationary mass	71.51 (48.76)	192.72	123.82	-
OIV occurs	51.66 (35.23)	100.59	92.13	2.11
Car stops	0	0	100.59	2.30
		Total	316.54	4.41

Table 3.2. Analytical model for 5004 lb pickup truck.

Instances	Speed of the truck, ft/s (mph)	K.E. of the truck (kip-ft)	ΔK.E. (kip-ft)	Displacement (ft)
Pre-impact	91.67 (62.5)	653.23	-	-
Impact with stationary mass	80.64 (54.99)	505.63	147.60	-
OIV occurs	56.67 (38.64)	249.65	255.98	3.41
Truck stops	0	0	249.65	3.33
		Total	653.23	6.74

These analytical models will differ from finite element models as well as experimental results because several factors are not considered. The displacement of the

vehicle due to frontal crush is not considered. This will have an effect in energy absorption during the initial collision. Also, the frontal crush of different vehicles is dependent on their crashworthiness, which varies greatly. Deceleration is considered constant which is not the actual case- it is a pulse with intermittent peaks. Analytical models can be used to compare with finite element models and experimental results to analyze the physical behavior of the designed TMA.

3.2. TMA Design

The final design parameters have been obtained through a series of development and analysis of finite element models. Scores of iterations were made in the design of the TMA based on required performance characteristics, which are defined by the energy dissipation efficiency, occupant safety, material and cost, and simplicity of the design for ease of manufacture. The designed TMA consists an assembly of rectangular steel tubes, an impact head, tube folders called squeezers, and outlet pipes to guide the folded tubes safely towards the ground.

Figure 3.1 shows 3-D model of the designed TMA. The components of the TMA are built using ASTM A36 steel. The nominal cross-section of the steel tubes used in the design is 6 in x 4 in. These folding tubes have three different wall thicknesses along their length- 10 gauge (0.140625 in) for the first 4.5 feet, 0.25 in for the next 2 feet, and 0.3125 in for the last 4.5-foot section. The impact head is made of C 6 x 8.2 channels with web thickness of 0.2 in, and 2 x 2 in square tubing with wall thickness of 0.1875 in as vertical and horizontal members. The length of the folding tubes used is 11 feet. The size of the impact head is 5 ft x 2 ft. The squeezer has wedges that cause the tubes passing through

them to ‘kick-in’, and the tapered section in the squeezer further deforms the tubes to fold them. The outlet pipe is elliptical in shape and consists of two sections of 15-inch long pipes bent with a radius of 25 inches. They guide the folded tubes safely towards the ground as well as act as an additional source of energy dissipation when the folded tubes are forced through their curvatures. The outlet pipes will be constrained on the docking station. The initial design idea is to have the lifting mechanism rotate the TMA about the squeezers so that the squeezers and outlet pipes have a separable connection. When the TMA is lowered, the openings on the squeezers align to the openings on the outlet pipes.

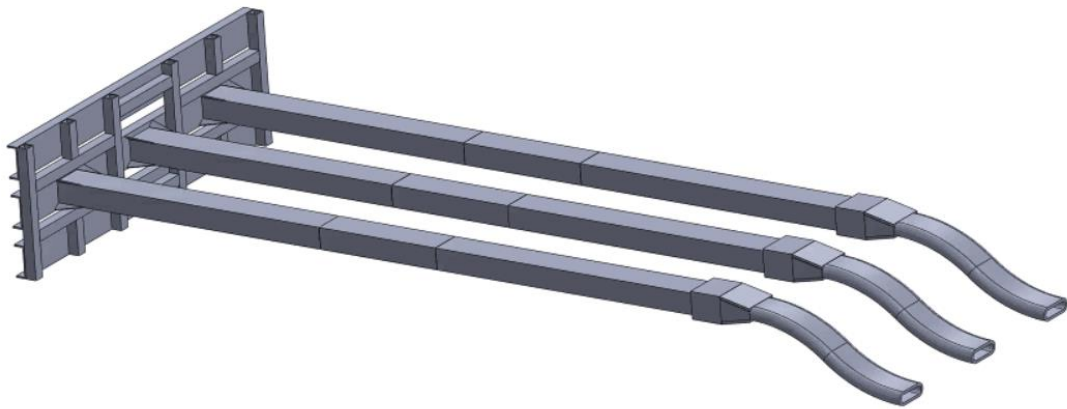


Figure 3.1. 3-D model of the designed TMA.

Figure 3.2 shows the arrangement of wedges inside the squeezer. The wedges are 5 inches long and 1.5 inches wide with a thickness of 0.25 inch. The squeezer is 12 inches long and is made of 0.5-inch thick steel plates welded together. Figure 3.3 shows the 3-D model of the impact head. The impact head acts as a source of dissipation of kinetic energy of the vehicle during initial impact, and also functions as a mechanical interlock to engage

the vehicle throughout the duration of collision. Design evaluations and parametric study through numerical modeling are discussed in detail in subsequent chapters in this report.

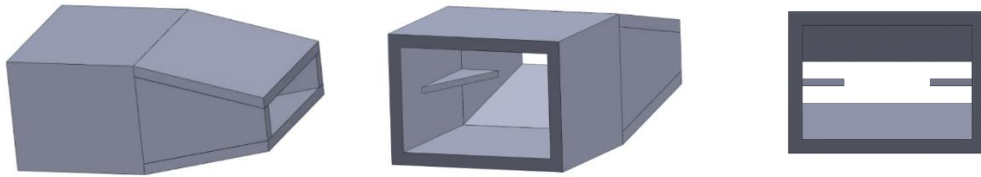


Figure 3.2. Squeezer tube with wedges welded horizontally.

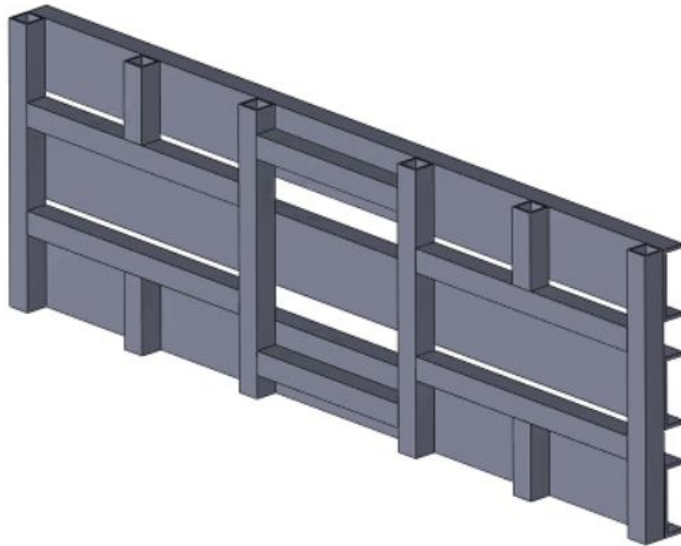
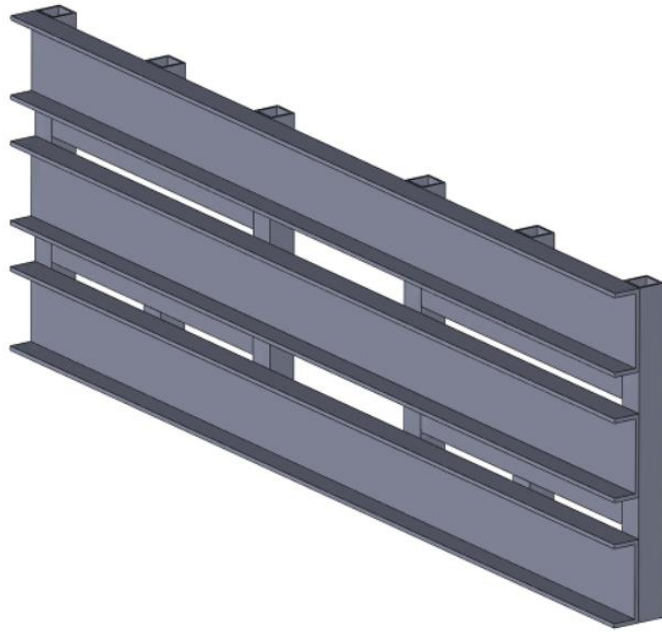


Figure 3.3. 3-D models showing front and back views of the impact head.

3.3. Numerical Model

Numerical modeling has developed over the years as a powerful tool for scientific research. Advancement in computational power of computers and continuous improvement in numerical techniques have made numerical modeling very reliable in the study of scientific problems. The non-linear finite element analysis code- LS-DYNA is used in this research study to develop numerical models to simulate impact of an errant vehicle with the designed TMA. Design of a highway safety feature is an iterative process which involves analysis and testing of candidate designs. Numerical models are extremely useful in evaluation of candidate designs to determine which design best meets the stability and occupant risk criteria mandated by MASH. Numerical modeling eliminates the requirement of repeated full-scale crash testing for each candidate design and for varying test conditions. Numerical models however will require validation from full-scale crash testing. Once validated from experimental results, numerical models can provide cost-effective, rapid and reliable solutions for a wide range of candidate designs and test conditions.

3.3.1 Material Model

Several material models are found in LS-DYNA that define material characteristics of a wide range of materials including metals, non-metals and polymers. For the design of the TMA, material model 3 (MAT_PLASTIC_KINEMATIC) in the LS-DYNA database- elastic plastic with kinematic hardening (also called plastic kinematic), is used to model the structural elements of the TMA. This model was developed by Krieg and Key in 1976. In this material model, a combination of isotropic and kinematic hardening may be

obtained by varying the parameter β between 0 and 1. This model is suited to model isotropic and kinematic hardening plasticity with the option of including rate effects. It is available for beam, shell and solid elements, and is very cost-effective (Livermore Software Technology Corporation, 2019).

Figure 3.4 shows kinematic and isotropic hardening obtained for values of β between 0 and 1. The parameters l_0 and l are the undeformed and deformed length of a uniaxial test specimen respectively. The stress and strain in the plot are true stress and true strain.

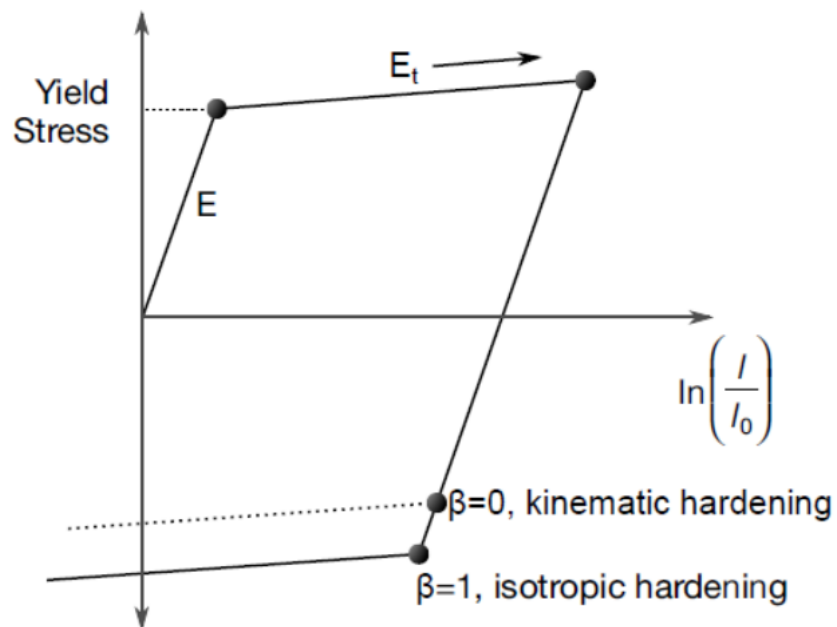


Figure 3.4. Elastic-plastic behavior with isotropic and kinematic hardening.

(Livermore Software Technology Corporation, 2019)

There are more accurate material models such as MAT_PIECEWISE_LINEAR_PLASTICITY available in LS-DYNA but they require stress-strain curves as input as well as more run time. The plastic-kinematic model is acceptable for the initial study of the TMA design, but more representative material models should be selected for future developments. Table 3.3 lists the material properties used in the development of finite element models in this research study.

Table 3.3. Properties of material used in the finite element models.

Material properties	Input values	Units
Density	7.32 e-4	lbf-s ² /in ⁴
Young's modulus of elasticity	3e7	psi
Poisson's ratio	0.3	-
Yield strength	36000	psi

CHAPTER 4- FINITE ELEMENT MODELING

4.1. Basic Finite Element Model

Figure 4.1 shows a basic finite element model of the tube folding mechanism. The solid model is developed in SOLIDWORKS. The model is discretized into finite elements using the HyperMesh software. The finite element model is developed using LS-PrePost and solved with the aid of UAB high performance research computing.

In the single-tube model shown in Figure 4.1, an errant car/ pickup-truck was simulated using a rigid plate having velocity equal to that of the errant vehicle- 90.93 ft/s (62 mph), and with one-third the mass of the errant vehicle- 808 lb (366.67 kg) for the small car and 1668 lb (756.67 kg) for the pickup truck. This was done to get an idea of the total stroke length required to bring the small car and pickup truck to a stop. The tube and rigid plate were meshed using shell elements, while the squeezer and wedges were meshed using solid elements. The element size for the tube was chosen to be 0.1875 inch, and element sizes for the squeezer and wedges were set to 0.0625 inch.

The model was run by varying static and dynamic friction coefficients (μ_S and μ_D) between components of the TMA. The thickness of the tube was also varied to determine the average force produced by tubes of different wall thicknesses. Since the designed TMA needs to stop vehicles with different masses (the pickup truck has more than twice the mass of the small car), a combination of two wall thickness was used in the tube. The first section

has a thinner wall section and the second section has a thicker wall section. In doing so, there exists the possibility of stopping both the small car and pickup truck within a reasonable stopping distance. A stroke length of 10 feet per folding tube was chosen as a reasonable length of the TMA to start with, for compact design and low material cost as well as to reduce vibrational loads and bending effects on tubes upon impact.

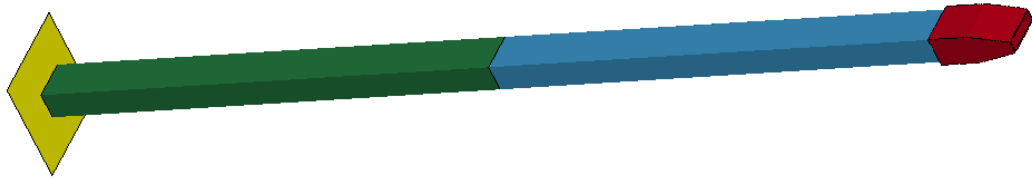


Figure 4.1. Basic finite element model of the tube folding mechanism.

The kinetic energy of the small car and pickup truck (considering one-third mass) travelling at a speed of 90.93 ft/s, and the average force required to be developed by the TMA to bring them to stop are estimated below.

$$(a) \text{ Mass of the small car} = 25.13 \text{ lbf-s}^2/\text{ft} \text{ (808 lb)}$$

$$\text{Velocity of the small car} = 90.93 \text{ ft/s}$$

$$\begin{aligned} \text{K.E. of the small car} &= \frac{1}{2} \times 25.13 \times (90.93)^2 = 103890.75 \text{ lbf-ft} \\ &= 103.89 \text{ kip-ft} \end{aligned}$$

Displacement of the car after impact with the TMA before coming to a stop = 10 feet

$$\begin{aligned} \therefore \text{Average force required to bring the car to a stop} &= \frac{\text{total kinetic energy}}{\text{total displacement}} \\ &= 10389.08 \text{ lbf} = 10.39 \text{ kip} \end{aligned}$$

(b) Mass of the pickup truck = 51.79 lbf-s²/ft (1668 lb)

Velocity of the pickup truck = 90.93 ft/s

$$\begin{aligned} \text{K.E. of the pickup truck} &= 1/2 \times 51.79 \times (90.93)^2 = 214106.72 \text{ lbf-ft} \\ &= 214.11 \text{ kip-ft} \end{aligned}$$

Displacement of the truck after impact with the TMA before coming to a stop = 10 feet

$$\begin{aligned} \therefore \text{Average force required to bring the truck to a stop} &= \frac{\text{total kinetic energy}}{\text{total displacement}} \\ &= 21410.67 \text{ lbf} = 21.41 \text{ kip} \end{aligned}$$

The basic finite element model was run for different coefficients of static and dynamic friction (μ_s and μ_d) between the components and different wall thickness of the tubes. The model was run by providing the impacting rigid plate one-third of mass and equal velocity of the pickup truck- 1668 lb and 90.93 ft/s. Figures 4.2 and 4.3 show the average force produced by the tube with wall thicknesses of 12 gauge (0.109375 in) and 10 gauge (0.140625 in); and of 10 gauge and 7 gauge (0.1875 in) respectively. As seen from the force plots, the forces produced by the tubes increases with increasing wall thickness and increasing friction in the model. The average forces produced by the tubes in the two models are listed in Table 4.1. These values are below the value of force required to bring the pickup truck to a stop (21411 lbf).

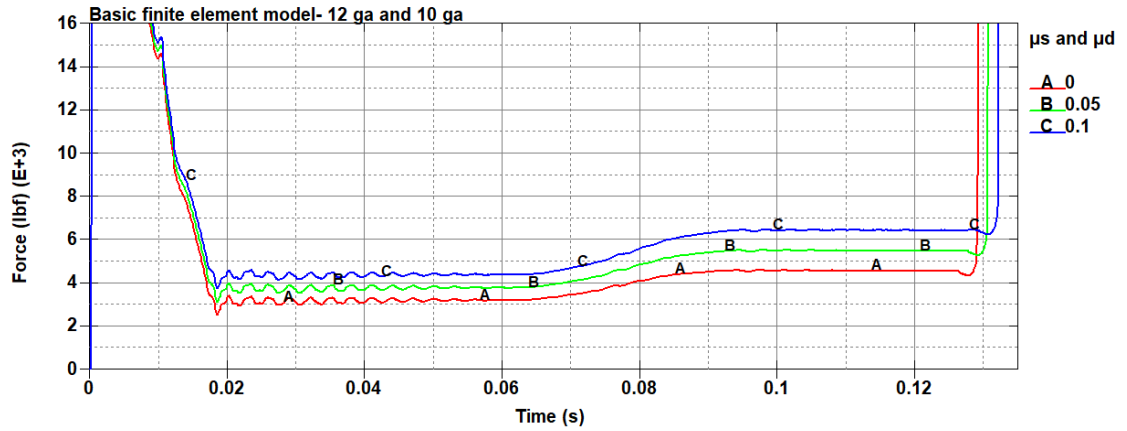


Figure 4.2. Force produced by the tube with wall thicknesses 12 gauge and 10 gauge.

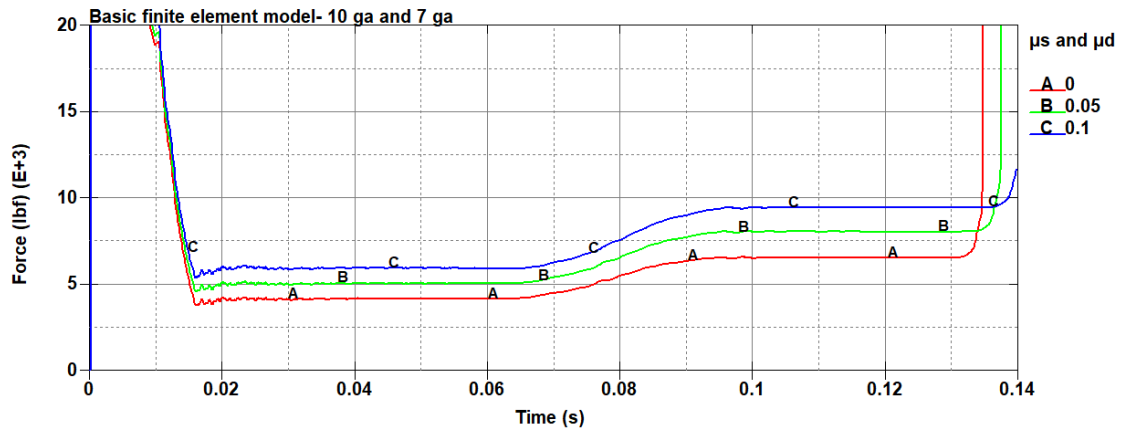


Figure 4.3. Force produced by the tube with wall thicknesses 10 gauge and 7 gauge.

Table 4.1. Forces produced in the models with different tube thicknesses.

μ_s and μ_d	12 ga and 10 ga model		10 ga and 7 ga model	
	Average force (lbf)		Average force (lbf)	
	12 ga section	10ga section	10 ga section	7 ga section
0	3210	4510	4140	6520
0.05	3790	5450	5030	8040
0.1	4400	6380	5920	9450

Since the forces produced by the tube with a combination of wall thicknesses of 12 gauge and 10 gauge, and of 10 gauge and 7 gauge, were not sufficient to bring both the small car and pickup truck to a stop, various changes were made to develop a working model. An impact head was added, tube wall thicknesses were increased, and outlet pipes were added. Numerous models were subsequently developed to account for different factors in the design so as to keep the OIV and RA values within the MASH recommended limits for tests 3-50, 3-51, 3-52 and 3-53. Some important subsequent models developed in this research study are described in the following sections.

4.2. Progression of Finite Element Models

4.2.1 Mesh Resolution Study

Mesh resolution study was conducted to determine the optimum mesh size of the folding tubes for the desired accuracy and run-time. The single-tube model described in section 4.1 was used to perform comparative study of the forces produced by the tube for various sizes of the shell elements. Figure 4.4 shows the forces produced by the tubes for

three mesh sizes- (a) 0.375 in, (b) 0.25 in and (c) 0.1875 in. The mesh size of the squeezer and wedges was kept a constant of 0.09375 in all three runs. The wall thickness of the tube was 10 gauge, and the impacting rigid plate was simulating the small car (test 3-50). Coefficients of static and dynamic friction (μ_s and μ_d) were assumed to be 0.05.

It can be seen in Figure 4.4 that there is convergence in results between mesh sizes of 0.25 in and 0.1875 in. Therefore, mesh size of 0.1875 in was chosen for shell section of the tube. The accuracy of a finite element analysis typically increases with finer mesh size, but this comes with an increase in run-time and cost. So, finer tube mesh sizes were discarded in this study and the shell sections of the tubes in all the subsequent models were assigned a mesh size of 0.1875 in (3/16") considering the computational efficiency and accuracy.

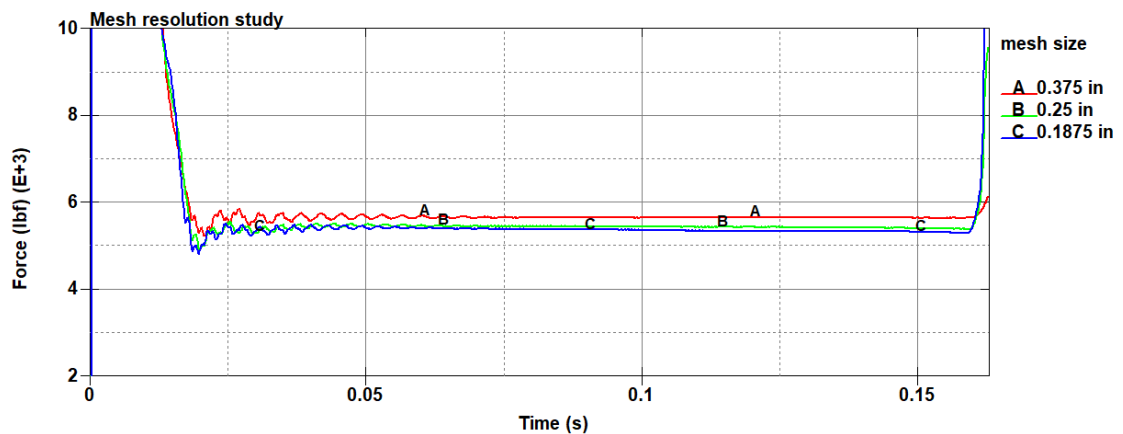


Figure 4.4. Forces produced by the tube for various mesh sizes

4.2.2. Parametric Study on Tube Wall Thickness

Effect of tube wall thickness in force developed and energy dissipated by the tubes was studied by developing a three-tubes model, with a basic impact head and impacting rigid plate. This model is shown in Figure 4.5. The model was run by providing the rigid plate the mass and velocity of the pickup truck- 5004 lb and 90.93 ft/s. The model was run for different wall thicknesses of the tubes ranging from 12 gauge to 0.3125 in. The length of the folding tubes was 138 in. The impact head was made of C 15 x 40 channels weighing 400 lb. The impact head was redesigned in the subsequent models and its mass was reduced. The thicknesses of the squeezer and wedges were 0.375 in and 0.25 in respectively. No friction was considered in the model.

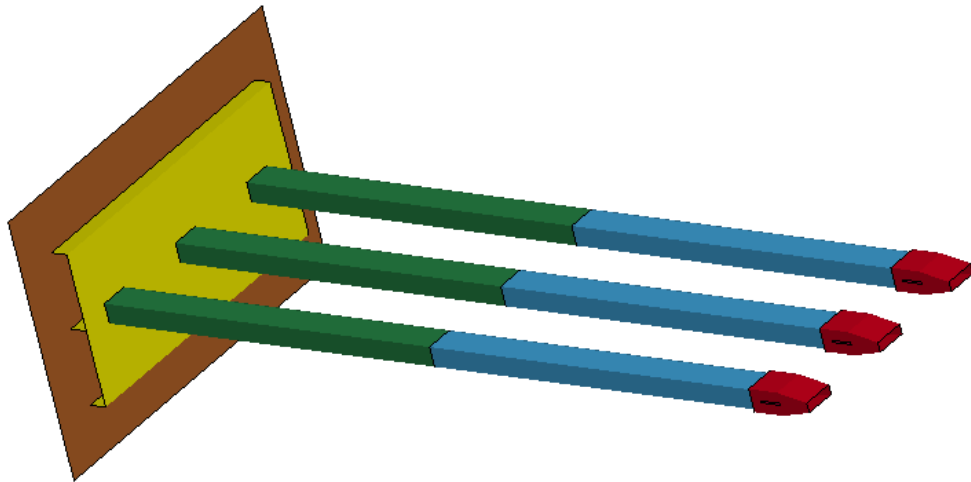


Figure 4.5. Three-tube model developed for study of the effect of tube wall thickness.

Plots of force acting on the impacting rigid plate with different tube wall thicknesses are shown in Figure 4.6. It is evident from the plots that as tube wall thickness

increases, the force produced by the tubes in decelerating the impact plate also increases. Table 4.2 lists the average force produced by the model with different wall thickness of the folding tubes. The tube with wall thickness of 0.3125 in is capable of producing about three times the force produced by the tube with wall thickness of 12 gauge (0.109375 in), and hence dissipates three times the kinetic energy of the impacting vehicle for same displacement.

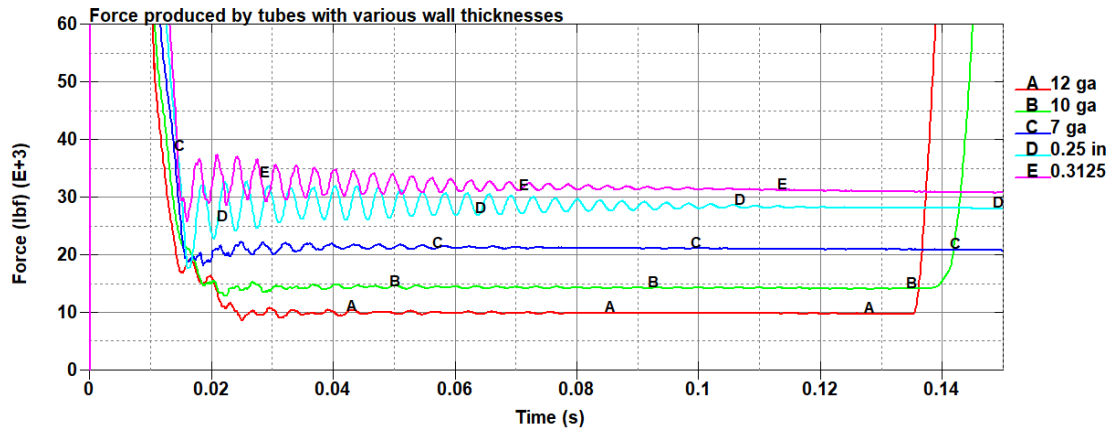


Figure 4.6. Force produced by tubes with various wall thicknesses.

Table 4.2. Average force produced by tubes with different wall thicknesses.

Tube wall thickness (in)	Average force produced (lbf)
0.109375	9840
0.140625	14300
0.1875	21000
0.25	28300
0.3125	31200

Plots of velocities and displacements over time for tubes with varying wall thickness are shown in Figures 4.7 and 4.8 respectively. The total displacement of the impacting rigid plate is about 142 inches which includes the width of the channels and the gap between the rigid plate and impact head. It can be seen from the velocity plots that as the tube wall thickness increases, the duration in which the total stroke of the tubes is achieved also increases. Also, due to the deceleration increasing with the increase in wall thickness of the tubes, the velocity at the end of the stroke is the lowest for the tube with 0.3125 in wall thickness.

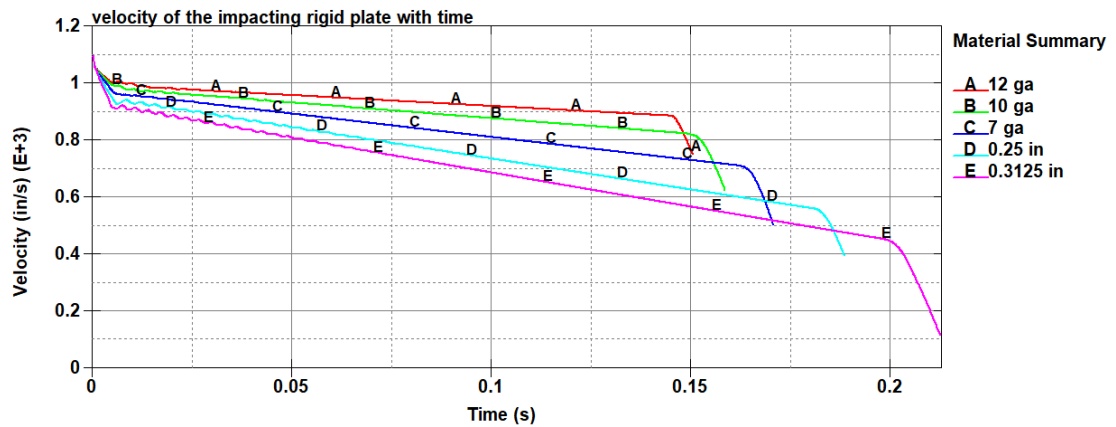


Figure 4.7. Velocity of the impacting rigid plate for different tube thicknesses.

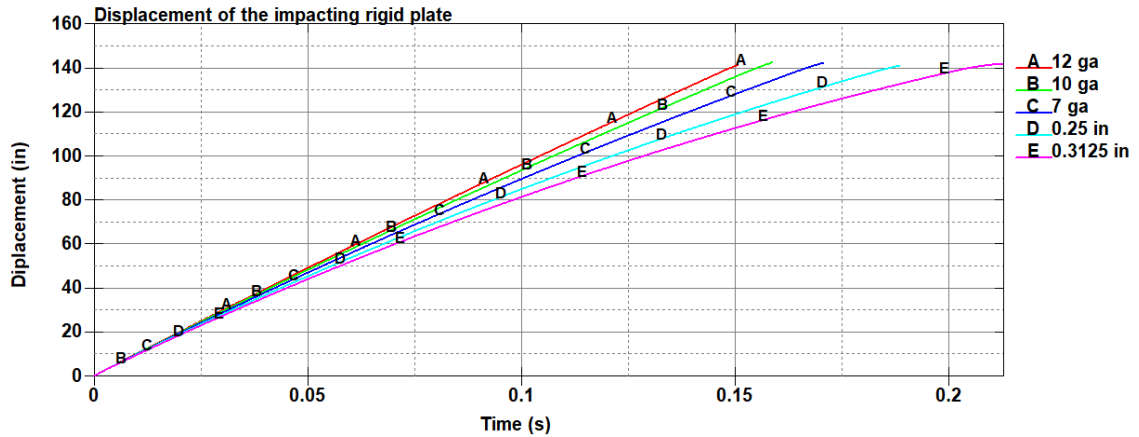


Figure 4.8. Plots of displacement for the impacting rigid plate with different tube thicknesses.

Plots showing the reduction in kinetic energy of the impacting rigid plate over time for models with different tube wall thicknesses are shown in Figure 4.9. The kinetic energy is dissipated the most by the tube with the highest wall thickness- 0.3125 in. Table 4.3 shows the amount of kinetic energy of the rigid plate dissipated by different tube thicknesses. The heavy impact head plays a significant role in energy dissipation at the initial impact. So, the kinetic energies of the tubes are calculated after 2 feet of displacement of the rigid plate so as to reduce the effect of impact head on the energy dissipation calculation. The energy dissipation capacity of tubes with different wall thicknesses is compared after 2 feet of displacement. As seen from Table 4.3, the tube with wall thickness of 0.3125 in dissipates about 4 times the energy as dissipated by the tube with 12-gauge wall thickness, instead of three times as found from the force analysis. The fact that calculation of energy was done after 2 feet of displacement has skewed the results. Nevertheless, the effect of wall thickness of the folding tube on energy dissipation capacity of the designed TMA has been established by these results.

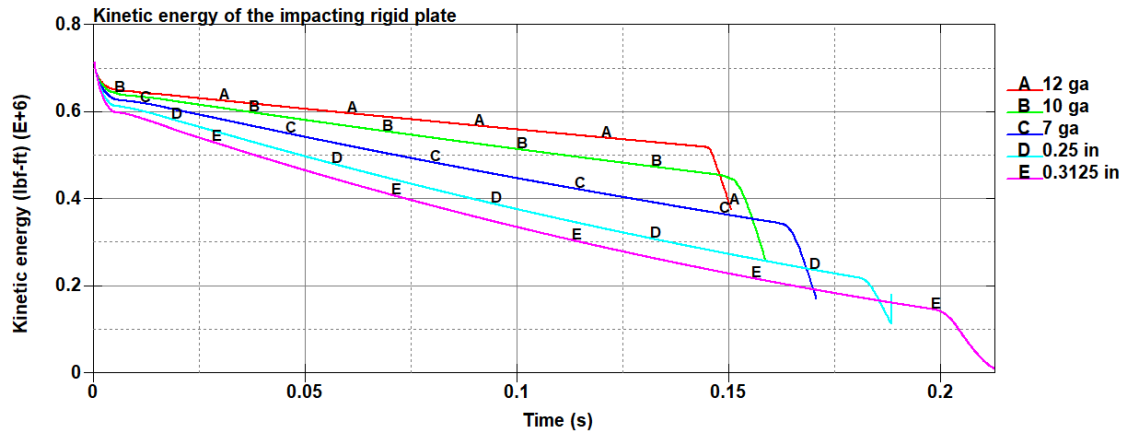


Figure 4.9. Kinetic energy of the rigid plate for tubes of various wall thicknesses.

Table 4.3. Kinetic energy of the rigid plate dissipated by tubes with different wall thicknesses.

Tube wall thickness (in)	Time corresponding to 2 ft of displacement (s)	Kinetic energy of the rigid plate after 2 ft of displacement (lbf-ft)	Final kinetic energy after complete stroke (lbf-ft)	% of kinetic energy of the rigid plate dissipated
0.109375	0.024	6.32e5	5.18e5	18.04 %
0.140625	0.0224	6.20e5	4.49e5	27.58 %
0.1875	0.025	5.93e5	3.40e5	42.66 %
0.25	0.0256	5.63e5	2.15e5	61.81 %
0.3125	0.0262	5.37e5	1.42e5	73.56 %

From the initial study of the single-tube model and the effect of tube wall thickness on energy dissipation, subsequent TMA models consisting of an impact head, three tubes-squeezer assemblies and outlet pipes were developed. Geometric properties and numerical

parameters were continuously varied in the finite element models for their comparative study. Although numerous models were developed and run in this study, only those which carry significant design information have been included here.

4.2.3. Model 1

Model 1 shown in Figure 4.10 consists of a rigid plate which was assigned a mass and velocity equal to that of the errant vehicle- 2425 lb and 91.67 ft/s in the case of the small car, and 5004 lb and 91.67 ft/s in the case of the pickup truck. The impact head, tubes, squeezers and outlet pipes were meshed using shell elements while the wedges were meshed using solid elements. Automatic single surface contact was set for all parts of the assembly, and for contact between the impact head and rigid plate, automatic one-way surface to surface tiebreak contact was imposed which ensured the impacting rigid plate and impact head remained in contact throughout the impact. The folding tubes in the model consisted of two different wall thicknesses along the length. The first section had a wall thickness of 7 gauge (0.1875 in) and the second section had a thickness of 0.25 in (1/4"). The shell sections of the impact head, squeezers and outlet pipes were assigned a thickness of 0.375 in (3/8"), while the wedges were 0.25 in (1/4") thick. The impact head had a size of 60 x 30 in. The outlet pipes were 36 inches long and 30 inches in height. The squeezers and outlet pipes were constrained in all translational and rotational directions to impose the boundary condition of a rigidly blocked support truck. The red and blue bands of nodes in Figure 4.10 are the constrained nodes of the squeezers and outlet pipes. The nodes are constrained in all translational and rotational directions.

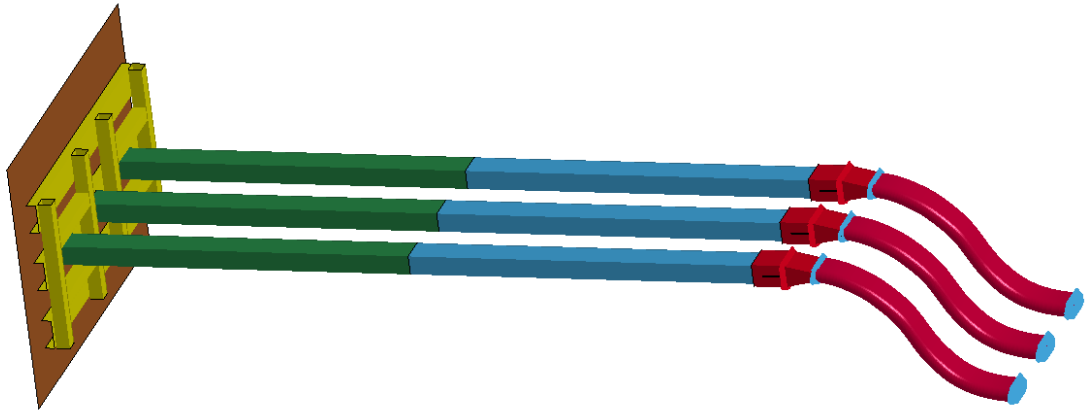


Figure 4.10. Three-tube model with a rigid plate simulated as the vehicle.

Figures 4.11 and 4.12 show rigid plate accelerations for test 3-50 and test 3-51 respectively. Initial spikes in acceleration can be seen from the figures that occur due to the initial impact between the vehicle and the impact head. This spike in acceleration occurs for a very short time period and is not of a concern because occupant impact with the vehicle interior occurs well past this initial impact. It can be seen from the plots that the 10-ms average peak occupant ride-down accelerations (RAs) for the small car model (test 3-50) for a range of coefficients of friction between TMA components are within the limit recommended by MASH- 659.25 ft/s² (20.49 g's). However, for the pickup truck model (test 3-51), the occupant ride-down accelerations (RAs) for friction coefficient 0.05 well exceeds the MASH recommended limits. For higher friction in the pickup truck model, the RA values fall within the limits. This is due to the fact that with higher friction in the model, more energy is dissipated throughout the stroke length and the truck has lesser energy at the end of the stroke when it strikes the constrained squeezer-outlet assembly. Table 4.4 tabulates the RA values for tests 3-50 and 3-51 for Model 1.

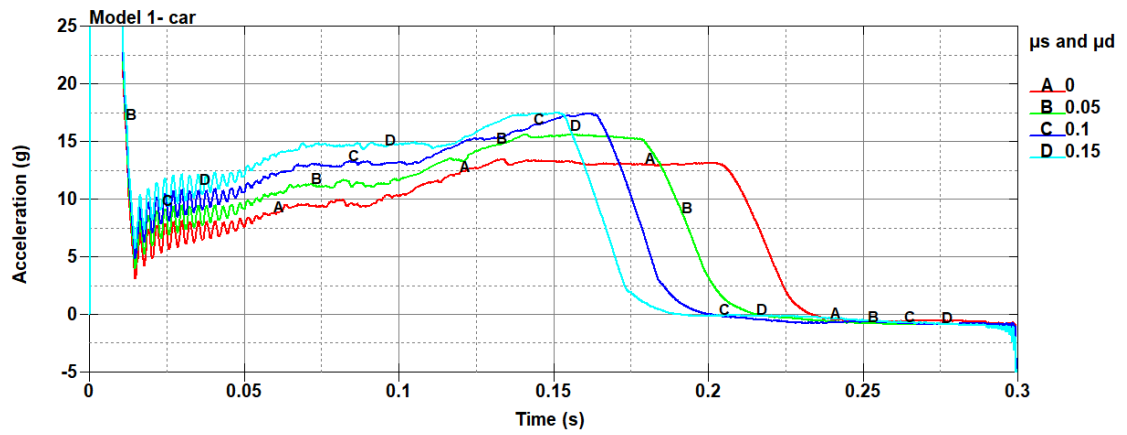


Figure 4.11. Accelerations from test 3-50 in Model 1.

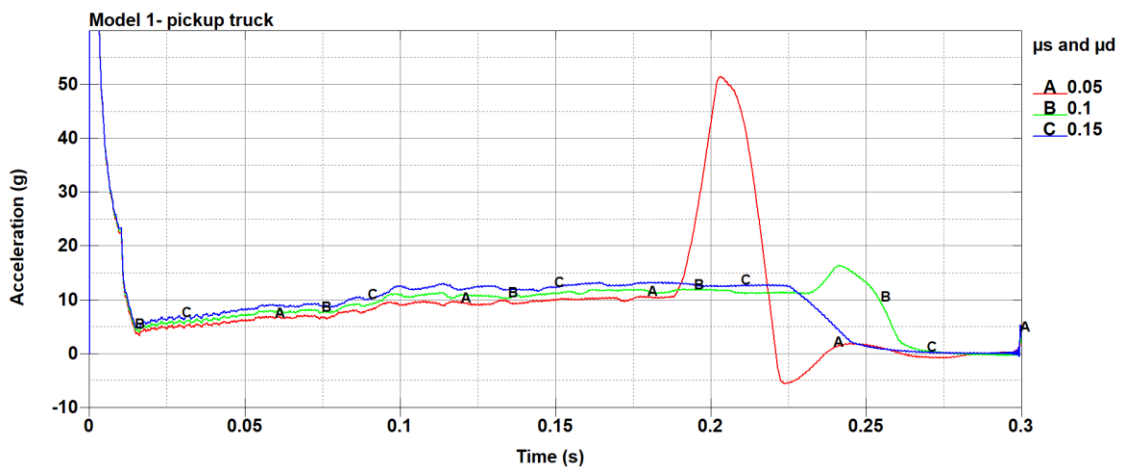


Figure 4.12. Accelerations from test 3-51 in Model 1.

Table 4.4. Occupant ride-down acceleration (RA) values for Model 1.

Test 3-50 (small car)		Test 3-51 (pickup truck)	
μ_s and μ_a	10 ms average peak RA (g's)	μ_s and μ_a	10 ms average peak RA (g's)
0	13.5	0	-
0.05	15.7	0.05	51.5
0.1	17.5	0.1	16.3
0.15	17.5	0.15	13.2

4.2.4. Model 2

After results suggested that the Model 1 was capable of bringing the small car to a stop within the recommended ride down acceleration (RA) limits, actual finite element models of the small car and pickup truck were obtained from the National Highway Traffic Safety Administration (NHTSA) website to be used in the TMA models. Models of a 2014 Chevrolet Silverado pickup truck (5004 lb mass), and a 2010 Toyota Yaris car (2425 lb mass) were used. Both vehicle models have velocity of 91.67 ft/s (62.5 mph). Figures 4.13 and 4.14 show the vehicle models assembled with the TMA model. A few changes were made to the TMA design while developing Model 2. The size of the impact head was reduced to 60 x 24 in. The size and curvature of the outlet pipes were changed- they consisted of 2 pieces 18 inches in length with a radius of curvature of 40 in. The TMA assembly was placed so as to maintain a distance of 15.75 in between the lower edge of the

impact head and the ground. The units in the TMA model were changed to ton, mm, s, N, MPa, N-mm units to match with those of the vehicle models.

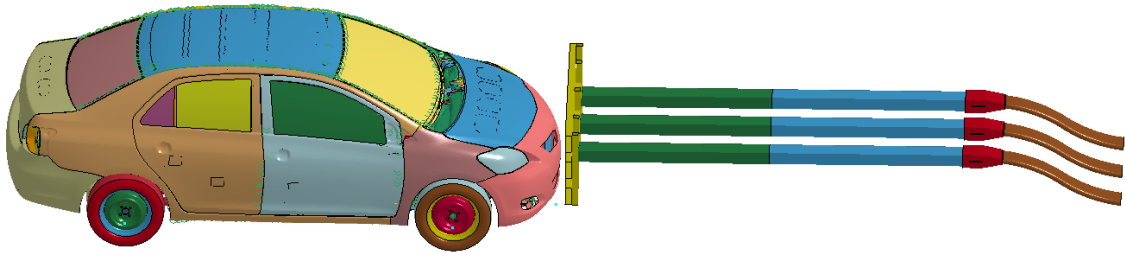


Figure 4.13. Finite element model simulating test 3-50 for the small car.

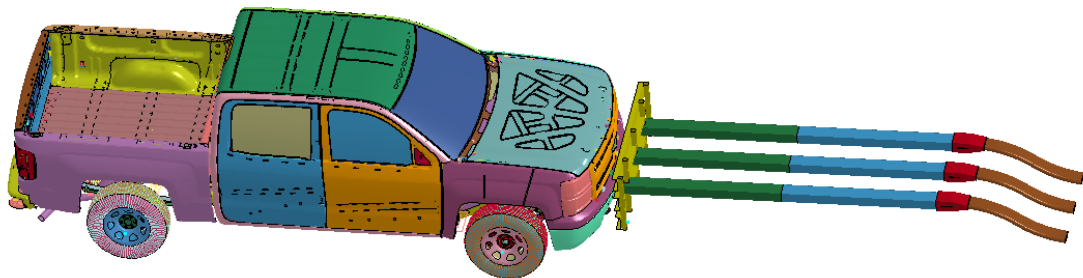


Figure 4.14. Finite element model simulating test 3-51 for the pickup truck.

Figure 4.15 shows the longitudinal accelerations occurring on the accelerometers of the car and the pickup truck. The 10-ms average peak accelerations for the car and

pickup truck models are 15.9 g's and 19.2 g's respectively, which differ from values in Table 4.4. This is due to the use of actual vehicle models instead of the rigid plate, as well as due to the change in size and curvature of the outlet pipes. Upon impact, the vehicle frontal area is subjected to substantial deformation, and contact between the vehicle and impact head also differs from that between the rigid plate and impact head.

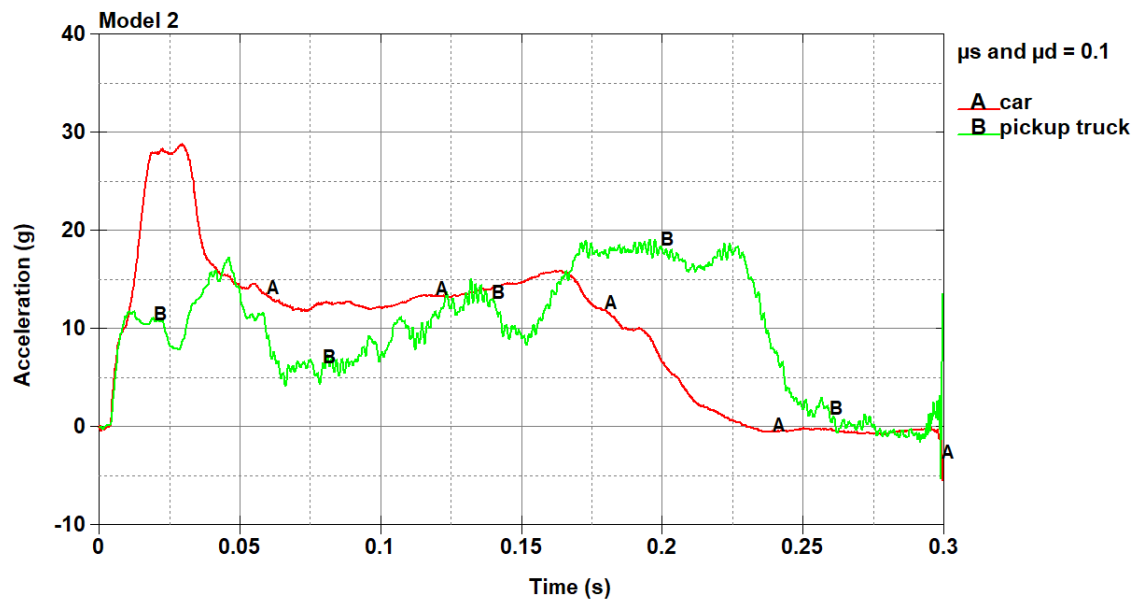


Figure 4.15. Longitudinal ride-down accelerations for tests 3-50 and 3-51.

Table 4.5 shows the calculation of longitudinal occupant impact velocities for tests 3-50 and 3-51. After impact with the TMA, the occupant continues travelling with the pre-impact velocity of 91.67 ft/s while the vehicular speed changes with time. At the instant when the occupant strikes the interior component of the vehicle, the relative displacement of the occupant with respect to the vehicle in the longitudinal direction is 2 feet. The occupant impact velocity is the relative speed of the occupant to the speed of the vehicle at this instant. It can be seen from Table 4.5, the occupant impact velocity for the car model is exceeding the limits recommended by MASH. This suggested that a tube with thinner

walls in the first section should be used in the TMA model. Also, the height of the impact head from the ground was a concern for the small car model. As can be seen from Figure 4.16, there was a possibility of the TMA running over the frontal face of the car which must be avoided. Taking all these things into consideration, Model 3 was subsequently developed which is described in the following section.

Table 4.5. Longitudinal OIVs for tests 3-50 and 3-51 for Model 2.

Test	μ_s and μ_d	Time (s)	Displacement of vehicle (ft)	Displacement of occupant (ft)	Velocity of the vehicle (ft/s)	OIV (ft/s)
3-50	0	0.0885	6.10	8.11	51.18	40.49
	0.1	0.0855	5.84	7.84	46.92	44.75
3-51	0.05	0.117	8.73	10.73	59.38	32.29
	0.1	0.113	8.37	10.36	58.40	33.27

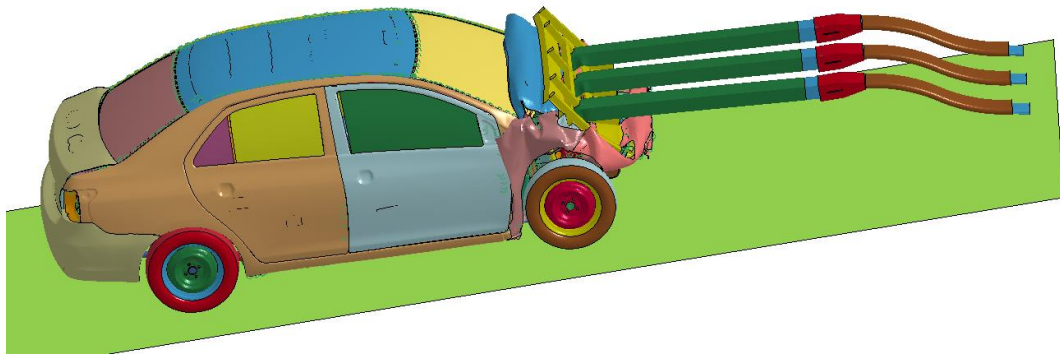


Figure 4.16. Test 3-50 showing the possibility of the TMA running over the car.

4.2.5. Model 3

Several further developments were carried out in the models to optimize the energy dissipation capacity of the TMA while keeping occupant safety criteria within the values recommended by MASH. As a result, Model 3 was developed using folding tubes with four different wall thicknesses along their length. The first 2.5-foot section had a wall thickness of 10 gauge (0.140625 in), the second 2.5-foot section had a wall thickness of 7 gauge (0.1875 in), the third 2.5-foot section had a wall thickness of 0.25 in, and the fourth 2.5-foot section had a wall thickness of 0.3125 in. The idea behind this was to control the OIV on the small car, while also providing more energy dissipation for the pickup truck towards the end of the stroke by adding a thicker section. Gussets of size 5 x 1.5 in and thickness of 0.1875 in were added at the folding tubes/impact head channels interface to provide more stability to the impact head. The distance of the lower edge of the impact head from the ground was reduced to 10 inches. The outlet pipes in Model 3 consist of two 15-inch sections with a radius of curvature of 25 inch. Figure 4.17 shows the 'four-thickness' TMA model, where the four sections are highlighted by color-coding.

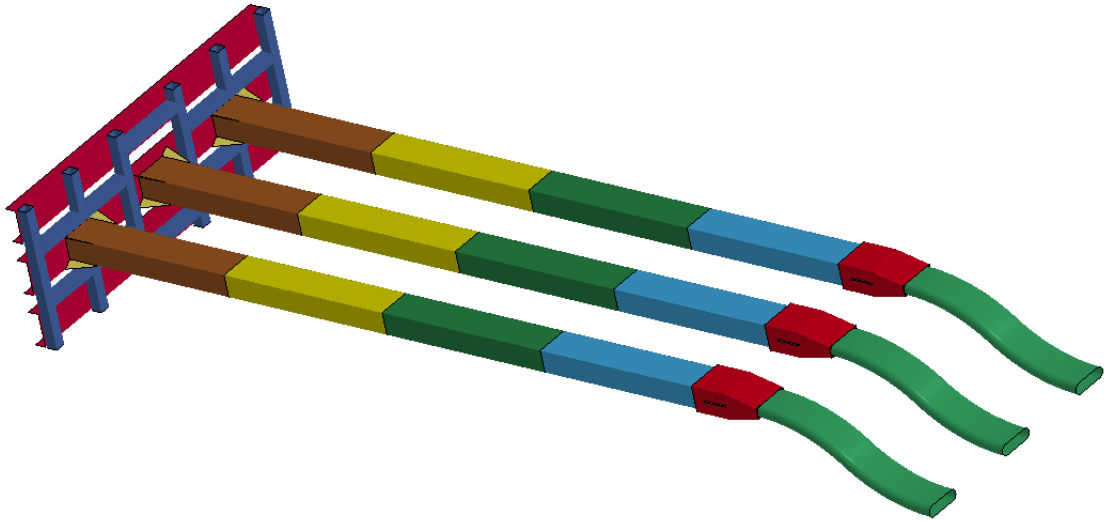


Figure 4.17. Model 3 with four wall thicknesses along the length of the tubes.

Figures 4.18 and 4.19 show the plots of longitudinal accelerations of the vehicular accelerometer for tests 3-50 and 3-51 respectively. The RA values are tabulated in Table 4.6. It can be seen that the occupant ride-down accelerations for test 3-50 are within the limits recommended by MASH but exceed the limits for test 3-51. This is due to the fact that sufficient energy dissipation was not achieved from folding of the tubes which caused the pickup truck to retain high kinetic energy at the end of the stroke, producing high deceleration when the truck gets stopped by the constrained squeezer-outlet assembly. The occupant impact velocities for both tests are shown in Table 4.7. It is evident that the OIV values for test 3-50 are close to/ exceeding the MASH limits. So, there was a need for lesser energy dissipation towards the first half of the stroke and more energy dissipation towards the second half of the stroke, corresponding to the small car and pickup truck respectively.

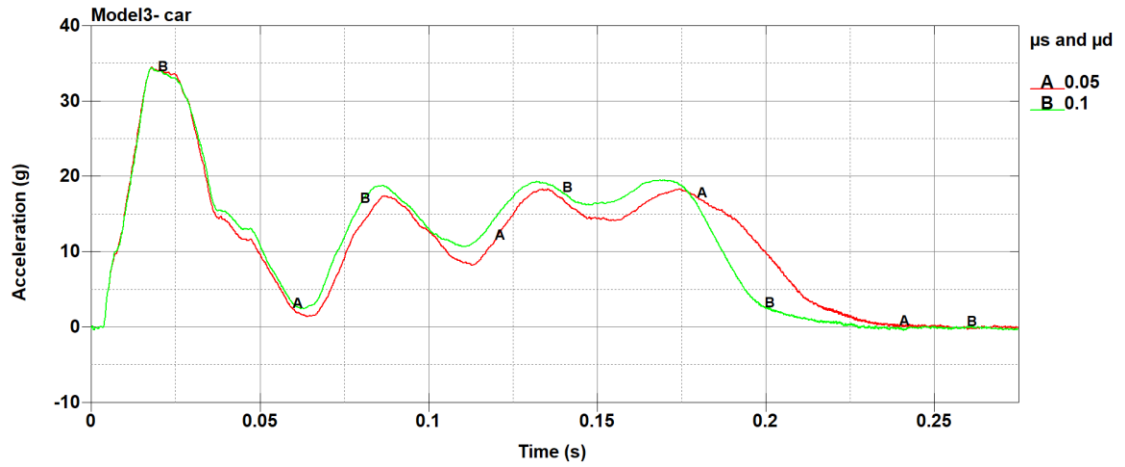


Figure 4.18. Longitudinal vehicular acceleration for test 3-50.

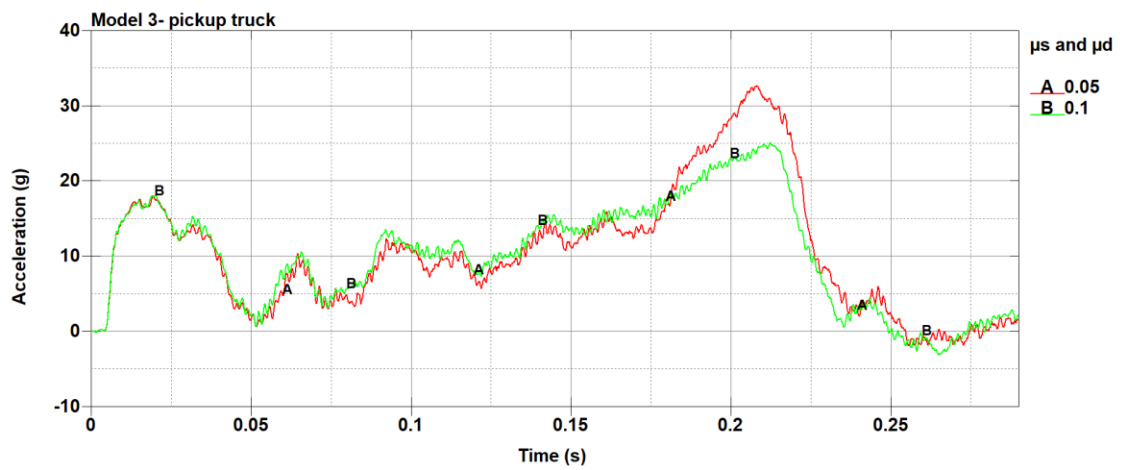


Figure 4.19. Longitudinal vehicular acceleration for test 3-51.

Table 4.6. Longitudinal occupant ride-down accelerations in Model 3.

Test 3-50 (small car)		Test 3-51 (pickup truck)	
μ_s and μ_a	10-ms average peak RA (g's)	μ_s and μ_a	10-ms average peak RA (g's)
0.05	18.3	0.05	32.7
0.1	19.5	0.1	25.1

Table 4.7. Longitudinal occupant impact velocities in Model 3.

Test	μ_s and μ_a	Time (s)	Displacement of vehicle (ft)	Displacement of occupant (ft)	Velocity of the vehicle (ft/s)	OIV (ft/s)
3-50	0.05	0.0848	5.77	7.77	51.84	39.83
	0.1	0.0842	5.71	7.72	49.54	42.13
3-51	0.05	0.113	8.37	10.36	60.37	31.30
	0.1	0.111	8.17	10.18	57.09	34.58

4.2.6. Model 4

Series of parametric studies were conducted by varying wall thickness of the tubes, mass and size of the impact head, and size and curvature of the outlet pipes. The length of the tubes was fixed to be 11 feet each considering the constraint on the length of the TMA,

to facilitate easy lifting and lowering of the unit, to avoid excessive vibration moments when employed, and to reduce bending of the tubes during offset and angular-offset impacts. After all the necessary geometric changes and parametric studies, the final finite element model of the TMA is produced. It is shown in Figure 4.20. The model consists of tubes with three different wall thicknesses. The first 4.5-foot section has a wall thickness of 10 gauge (0.140625 in); the second 2-foot section has a wall thickness of 0.25 in; and the third 4.5-foot section has a wall thickness of 0.3125 in. Shell sections of the squeezers and outlet pipes have a thickness of 0.5 in. The impact head is made of C 6 x 8.2 channel and 2 x 2 in square tubing. The position of impact head and the size and curvature of the outlet pipes are the same as Model 3.

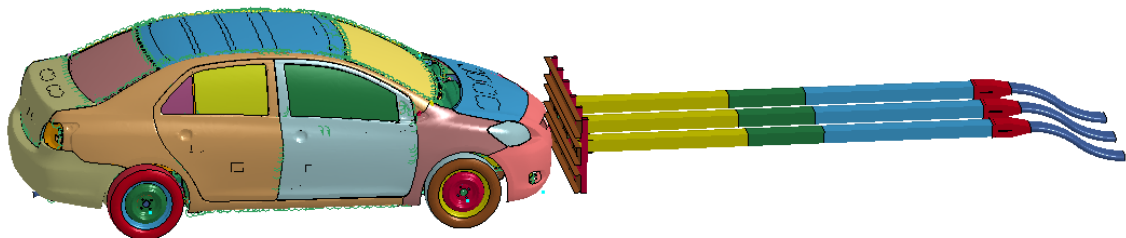


Figure 4.20. Final finite element model of the TMA consisting of tubes with three different wall thicknesses.

The developed finite element model is successful in dissipation of impact energy from tests 3-50 and 3-51 while keeping the OIV and RA requirements under the recommended values in MASH. For tests 3-52 and 3-53 (offset head-on impact and offset angular impact of the pickup truck), the model is behaving satisfactorily with a few

modifications in the design required for proper functioning of the TMA under those impact conditions. The results from all these tests are included in detail in the 'Results and discussion' section of the report.

4.2.7. Effect of Outlet Pipes

It has been found throughout the development of several models of the TMA that the outlet pipe has an effect on the energy dissipation capability of the TMA. The outlet pipe acts to direct the folded tubes safely towards the ground while also acting as an additional energy dissipation source in the TMA. When the folded tubes are forced through the curvature of the outlet pipes, they experience frictional forces and a 'kinking-effect' which aids in energy dissipation. The size and radius of curvature of the outlet pipes affect the energy dissipation through them. For the final finite element model, the outlet pipe consists of two sections of 15-inch long elliptical pipes with a radius of curvature of 25 inches. This design of the outlet pipes has been optimized during development of several finite element models. The effects of outlet pipes in energy dissipation has been studied by comparing the final finite element model with the outlet pipes to the one without the outlet pipes. The models are run by varying the coefficients of static and dynamic friction (μ_s and μ_d).

Comparison of kinetic energy of the vehicle are done for models with and without outlet pipes. For test 3-51 for pickup truck, Figure 4.21 shows the plots of kinetic energies for coefficient of static and dynamic friction of 0.05. It is evident from the plots that the outlet pipes are dissipating additional energy in the model with outlet pipes. Table 4.8 reflects the percentage of kinetic energy of the pickup truck dissipated by the effect of

outlet pipes for different coefficients of friction. The comparison of kinetic energy has been done at the instant when the stroke of the folding tubes is completed in either of the models. This has been termed ‘final K.E.’ in Table 4.8. It has been found that for lower coefficients of friction (0.05 and 0.1), the stroke of the tubes is completed first in the model without the outlet pipes; while for higher coefficients of friction (0.15 and 0.2), the stroke of tubes is completed first in the model with the outlet pipes.

About 10 % of kinetic energy of the impacting vehicle is dissipated by the outlet pipes in models with friction coefficients of 0 and 0.05, however this number falls to about 4% for the models with friction coefficients of 0.15 and 0.2. This might have been due to the fact that with higher friction in the model, a higher proportion of energy is dissipated by folding and squeezing of the tubes, and the contribution of the ‘kinking-effect’ by the outlet pipes is lower. Also, the fact that the entire stroke length of the tubes is not utilized in models with higher friction, where thicker sections of the tubes are not consumed completely, reduces the energy dissipation by the outlet pipes.

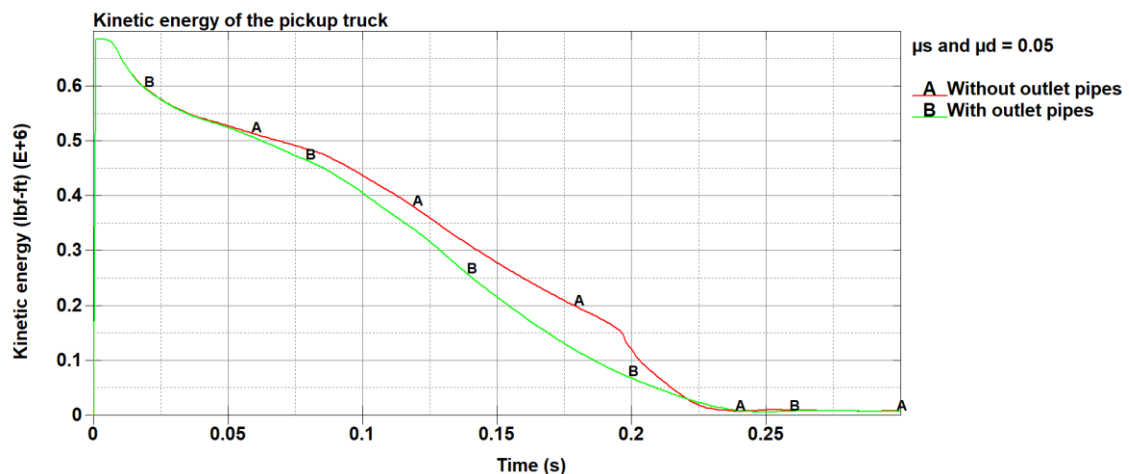


Figure 4.21. Kinetic energy of the pickup truck for study of effects of outlet pipes.

Table 4.8. Effect of outlet pipes in energy dissipation.

μs and μD	Initial K.E. (lbf-ft)	Final K.E. in model without outlet pipes (lbf-ft)	Final K.E. in model with outlet pipes (lbf-ft)	% of K.E. dissipated	
				Without outlet pipes	With outlet pipes
0.05	6.86e5	1.53e5	7.67e4	77.70	88.82
0.1	6.86e5	9.73e4	3.31e4	85.82	95.17
0.15	6.86e5	3.92e4	8.41e3	94.29	98.77
0.2	6.86e5	3.23e4	8.70e3	95.29	98.73

4.2.8. Effect of Mass of the Impact Head

The impact head plays an important role in the TMA function. Not only does it act as a mechanical interlock between the TMA and the impacting vehicle, it also acts as an additional source of dissipation of kinetic energy of the impacting vehicle. Several impact head designs were developed during the development of finite element models. The impact head used in the final model has a size of 60 x 24 in. It is made of 6 in channels and 2 x 2 in square tubing for vertical and horizontal support members. The thickness of the sections of the impact head channels and tubes were changed to vary the mass of the impact head and study its effect on the energy dissipation in the final model. The web thicknesses of the impact head channels and wall thicknesses of the tubes chosen for this analysis, and their mass, are shown below in Table 4.9.

Table 4.9. Mass of different impact heads considered.

S.N.	Channel web thickness (in)	Tube wall thickness (in)	Mass of the impact head (lb)
1.	0.140625	0.140625	133.20
2.	0.2	0.1875	183.62
3.	0.25	0.25	236.80

Figure 4.22 shows the vehicular accelerations for the pickup truck model (test 3-51) for the considered masses of the impact head. Coefficients of static and dynamic friction of 0.05 are considered in the model. It can be seen from the acceleration plots that an increase in mass of the impact head will increase the initial impulsive deceleration due to an increase in inertial effects. Also due to the heavier impact head dissipating more energy at the initial instant of impact, the occupant ride-down acceleration is lower at the end of the stroke, i.e. the pickup truck has less kinetic energy remaining at the end of the stroke length. The velocity plots for the three masses of impact heads also show that the loss of velocity at the beginning of collision is the most in case of the heaviest impact head, and the least at the end of the collision. The velocity plots are shown in Figure 4.23.

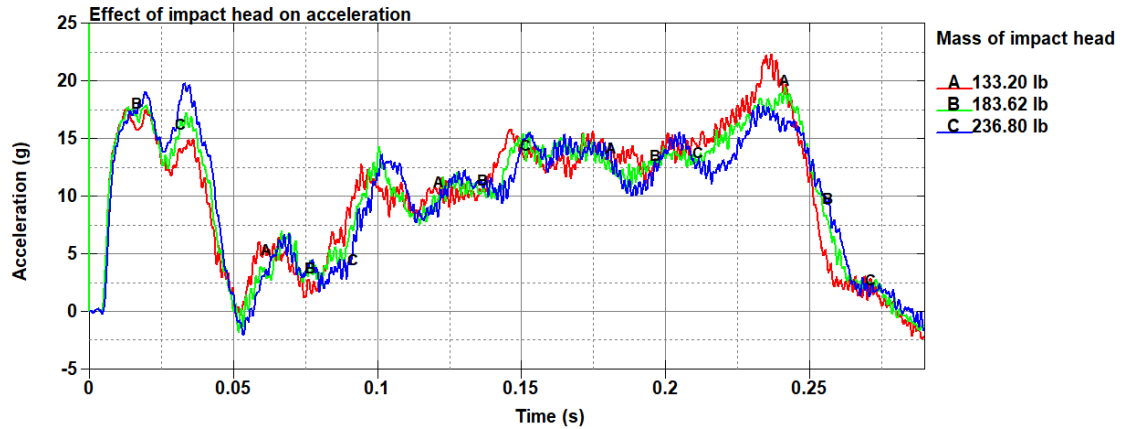


Figure 4.22. Effect of mass of impact head on vehicular accelerations.

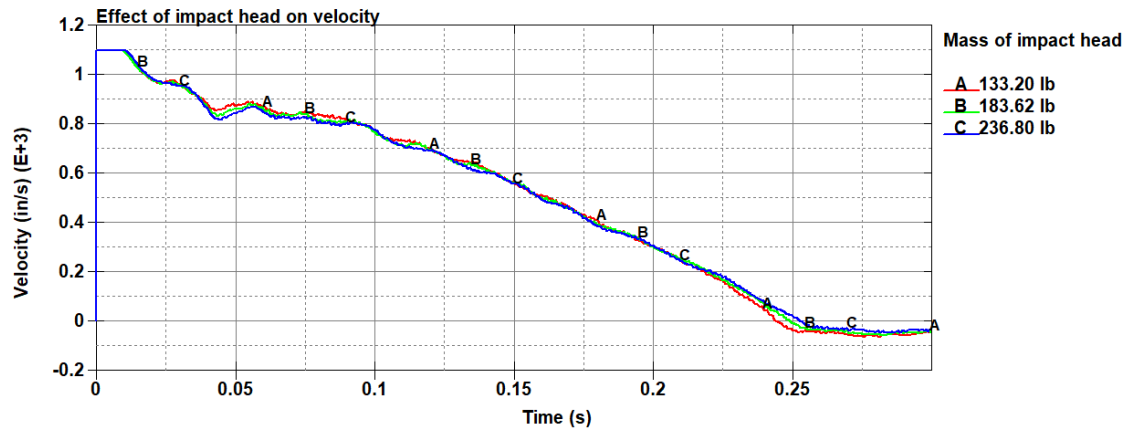


Figure 4.23. Effect of mass of impact head on vehicular velocities.

The 10-ms average peak occupant ride-down accelerations for the model analyzed for different masses of the impact head are shown in Table 4.10. It can be seen that due to more energy getting dissipated by the heavier impact head at the beginning of the collision, the peak ride-down accelerations occurring at the end of the energy dissipation process (end of the stroke) are lower for the model with the heavier impact head.

Table 4.10. Longitudinal occupant RA for models with different impact heads.

Test	μ_s and μ_d	Mass of impact head (lb)	10-ms average peak RA (g's)
3-51	0.05	133.20	22.3
		183.62	19.5
		236.80	18.0

The mass of the impact head has a strong effect in the occupant impact velocity (OIV) in the case of the small car model test (test 3-50). It has been found through series of finite element models in this study that an increase in mass of the impact head acts to increase the OIV on the small car model. So, taking all these factors into consideration, an impact head with mass of 183.62 lb, made of C 6 x 8.2 channels with web thickness of 0.2 inch and 2 x 2 in square tubing with wall thickness of 0.1875 in, has been selected to be used in the final model. Also, these are standard sizes of C channels and square tubing which are readily available from a fabrication point of view.

CHAPTER 5- RESULTS AND DISCUSSION

The final finite element model developed in this study (Model 4) has some changes in comparison to the previously developed models by taking a few factors into consideration. For tests 3-52 and 3-53 involving the pickup truck having an offset impact and offset angular impact respectively, the tubes got folded for a major portion of the impact before the tubes got bent due to lateral moment, causing them to lock up inside the squeezer. The squeezers and outlet pipes were also exhibiting plastic deformation due to the pressure exerted by the bent tubes. To counter this problem, the thickness of the squeezers and outlet pipes was increased to 0.5 in. Contact between the tubes and squeezers was improved by using ‘automatic nodes to surface contact’ while developing the numerical model in LS-DYNA. Despite these improvements in the model, perfectly working results have not been achieved for tests 3-52 and 3-53, which are areas for future research.

5.1. Sequential Images

Figures 5.1, 5.2, 5.3 and 5.4 show sequential images of impact for tests 3-50, 3-51, 3-52 and 3-53 respectively. For test 3-50, it can be seen that the energy of the impacting car is dissipated completely well before entire stroke length is reached. In test 3-51, the entire stroke length of the tubes is utilized before the pickup truck comes to stop. In test 3-

52, the tubes get locked up inside the squeezer and a large portion of the third section of the folding tubes does not contribute to energy dissipation. The situation is similar in test-53. The bending effects on the tubes can be reduced by using a longer squeezer section, however this will hinder the total stroke length of the folding tubes. If such change is made, a method to shear the additional length of the squeezer section should be devised to use the entire stroke length of the tubes for energy dissipation.

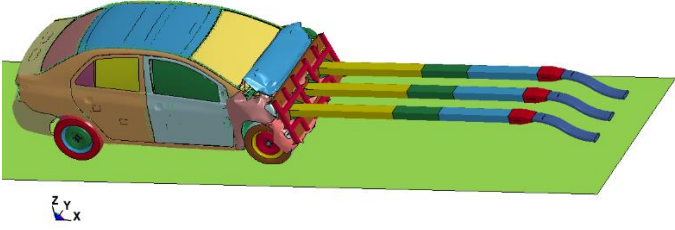
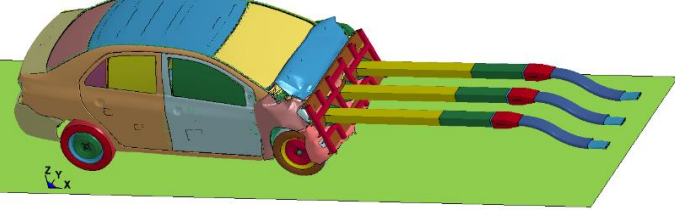
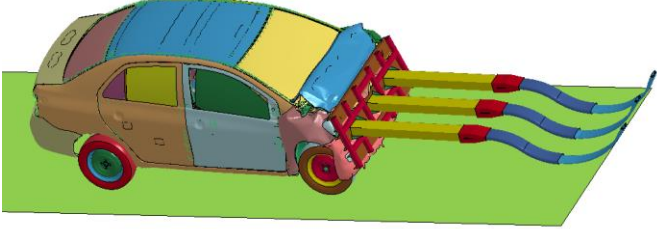
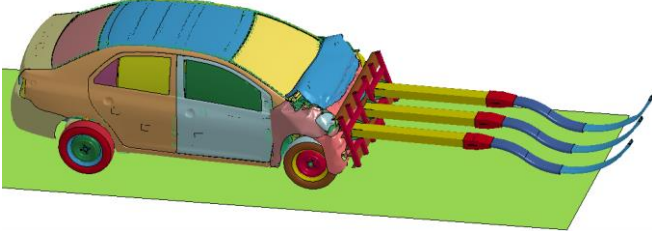
Time	Velocity	Sequential images
45 ms	59.05 ft/s	
100 ms	47.24 ft/s	
200 ms	1.03 ft/s	
300 ms	0	

Figure 5.1. Sequential images of test 3-50.

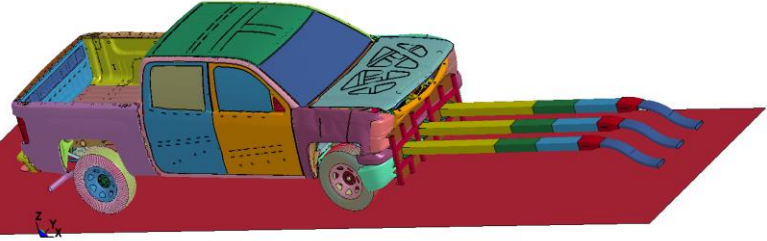
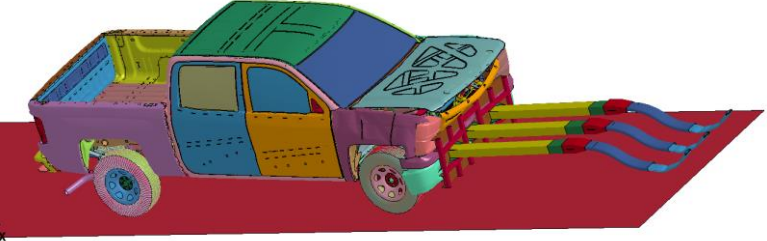
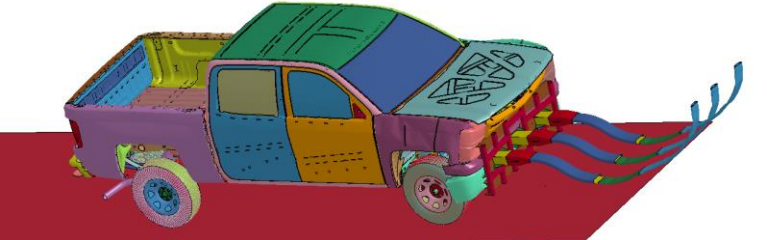
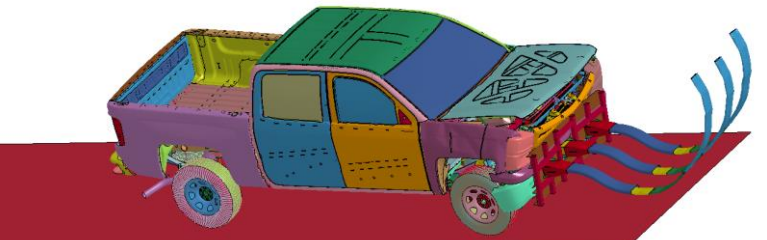
Time	Velocity	Sequential images
50 ms	71.85 ft/s	
100 ms	63.98 ft/s	
200 ms	28.78 ft/s	
300 ms	0	

Figure 5.2. Sequential images of test 3-51.

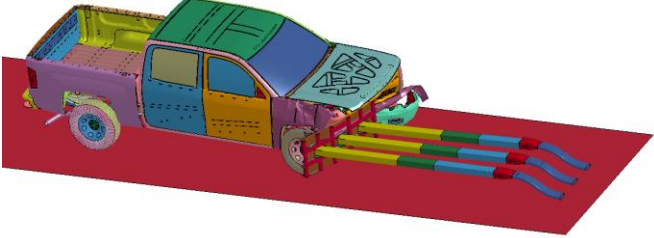
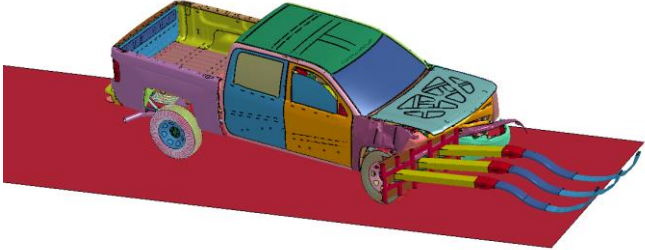
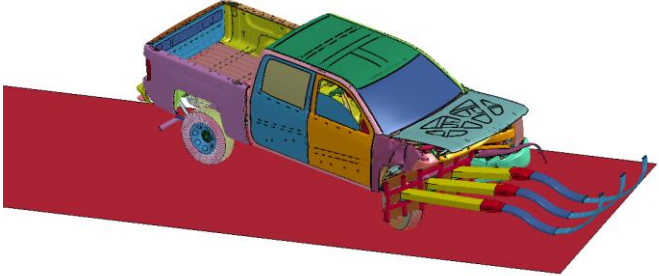
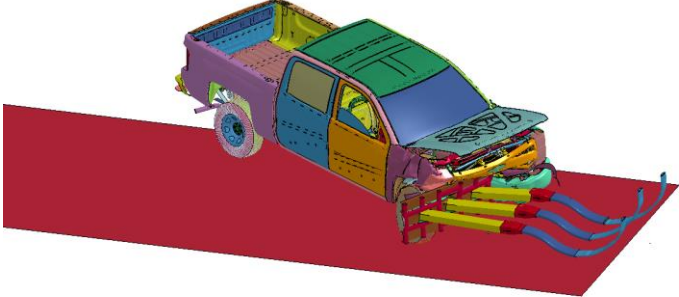
Time	Velocity	Sequential images
50 ms	74.48 ft/s	 <p>A 3D CAD model of a truck, viewed from a rear-quarter perspective, is shown on a red rectangular base. The truck is colored in various shades: purple for the body, green for the roof, blue for the windows, and yellow for the interior. At the rear, several colored tubes (yellow, red, blue) are attached, extending backwards and slightly downwards. The truck is positioned on a red surface that appears to be a ramp or a test track.</p>
150 ms	49.21 ft/s	 <p>A 3D CAD model of the same truck, viewed from a rear-quarter perspective, is shown on a red rectangular base. The truck is colored in various shades: purple for the body, green for the roof, blue for the windows, and yellow for the interior. At the rear, several colored tubes (yellow, red, blue) are attached, extending backwards and slightly downwards. The truck is positioned on a red surface that appears to be a ramp or a test track.</p>
200 ms	12.60 ft/s	 <p>A 3D CAD model of the same truck, viewed from a rear-quarter perspective, is shown on a red rectangular base. The truck is colored in various shades: purple for the body, green for the roof, blue for the windows, and yellow for the interior. At the rear, several colored tubes (yellow, red, blue) are attached, extending backwards and slightly downwards. The truck is positioned on a red surface that appears to be a ramp or a test track.</p>
250 ms	0.22 ft/s	 <p>A 3D CAD model of the same truck, viewed from a rear-quarter perspective, is shown on a red rectangular base. The truck is colored in various shades: purple for the body, green for the roof, blue for the windows, and yellow for the interior. At the rear, several colored tubes (yellow, red, blue) are attached, extending backwards and slightly downwards. The truck is positioned on a red surface that appears to be a ramp or a test track.</p>

Figure 5.3. Sequential images of test 3-52.

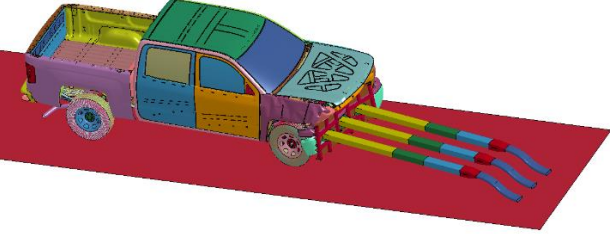
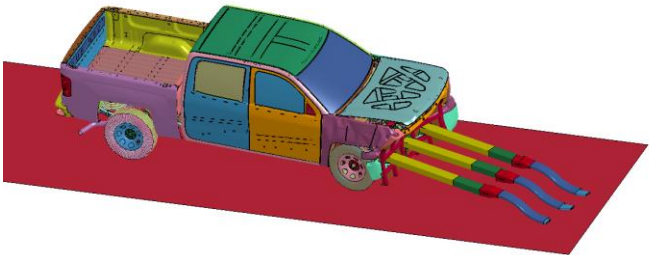
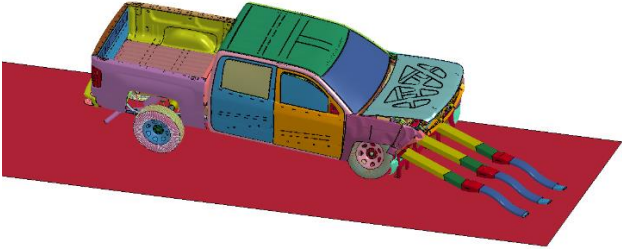
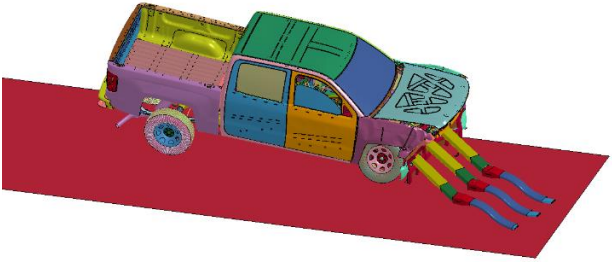
Time	Velocity	Sequential images
50 ms	73.16 ft/s	
100 ms	55.12 ft/s	
150 ms	5.65 ft/s	
200 ms	5.87 ft/s	

Figure 5.4. Sequential images of test 3-53.

5.2. Results for Test 3-50

Figure 5.5 shows the acceleration for test 3-50 with the small car for different values of coefficients of static and dynamic friction in the model. It can be seen that as friction increases, the deceleration of the car increases, producing higher average forces in the system.

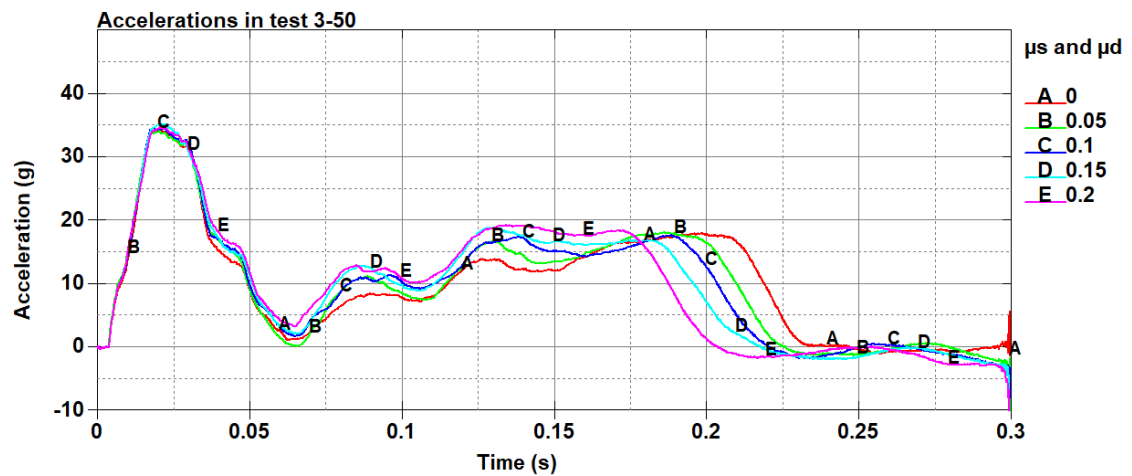


Figure 5.5. Accelerations in the small car model for different coefficients of friction.

Velocity and displacement plots for test 3-50 are shown in Figures 5.6 and 5.7 respectively. The car comes to a stop in all models. As friction increases in the model, total displacement of the car decreases.

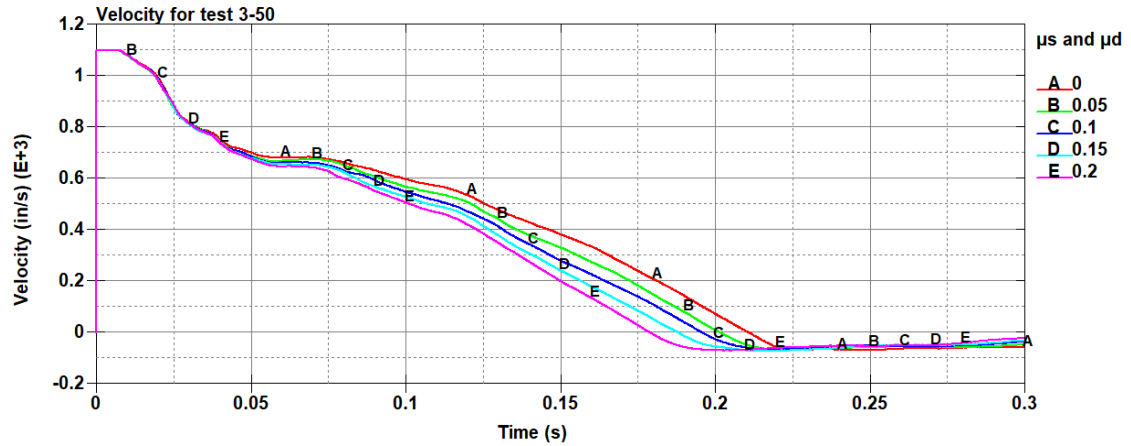


Figure 5.6. Velocity plots for the car model for different friction coefficients.

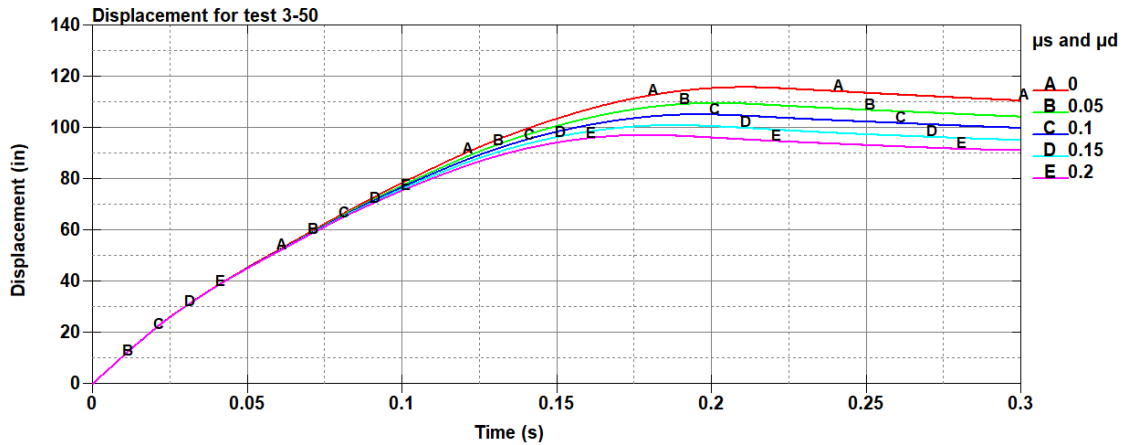


Figure 5.7. Displacement of the car with time for different coefficients of friction.

Average forces produced in the small car model for varying friction have been reported in Table 5.1. The average forces produced in the system increase from 34 kip to 40.5 kip when the coefficients of static and dynamic friction are varied from 0 to 0.2.

Table 5.1. Average forces produced in the model for test 3-50.

μ_s and μ_d	Initial K.E. (lbf-ft)	Final K.E. (lbf-ft)	ΔK.E. (lbf-ft)	Total displacement (ft)	Average force (lbf)
0	3.30e5	2.43e3	3.28e5	9.65	33990
0.05	3.30e5	2.41e3	3.28e5	9.12	35965
0.1	3.30e5	2.51e3	3.27e5	8.76	37329
0.15	3.30e5	2.01e3	3.28e5	8.43	38909
0.2	3.30e5	1.87e3	3.28e5	8.10	40494

Figure 5.8. shows the energy for test 3-50. The hourglass energy in the model is negligible which is always desirable in finite element models. The kinetic energy of the system decreases with time because of gradual loss of speed due to energy dissipation. This loss in kinetic energy results in a rise in internal energy with time. The sliding interface energy increases with time and becomes constant after the car stops. After 200 ms of run-time when the car stops, there is an increase in the internal energy (and as a result total energy), which is an anomalous behavior. After careful investigation of the simulation, it has been found that this occurs because the car after stopping, retreats backwards and pulls the impact head which is bound to it. This pulls the folded tubes along with the impact head and hence causes the rise in internal energy. The results up to 200 ms appear to be reasonable and do not alter the conclusions given above.

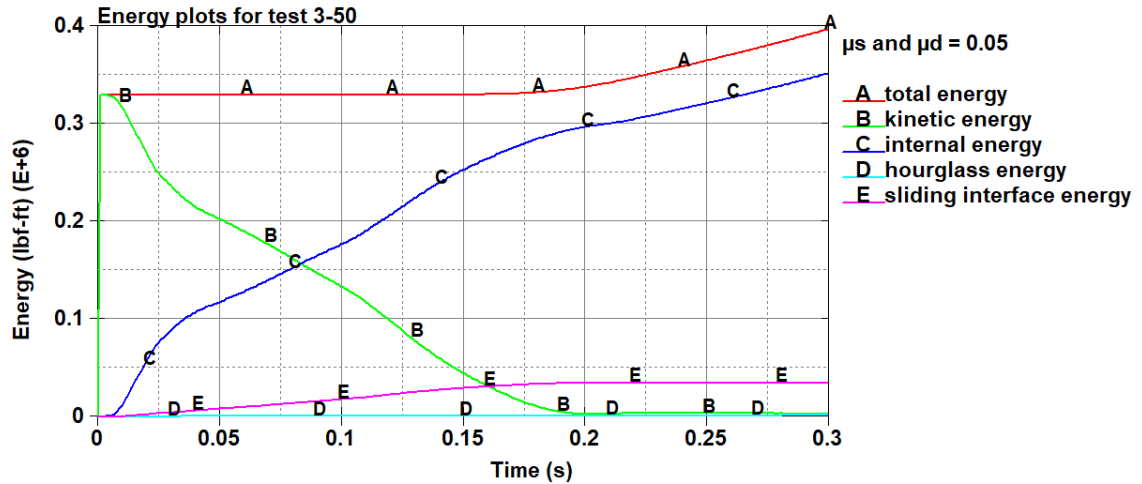


Figure 5.8. Energy balance for test 3-50.

5.3. Results for Test 3-51

Figure 5.9 shows the acceleration for test 3-51 with the pickup truck for different values of friction coefficients. As friction increases, the deceleration of the truck increases, producing higher average forces in the system. The stroke length of the tubes in the model is consumed completely for lower coefficients of friction, and for higher coefficients of friction, the stroke length in the model is sufficient for bringing the pickup truck to a stop. Because of this, for lower coefficients of friction, there is high acceleration at the end because the pickup truck still carries substantial kinetic energy.

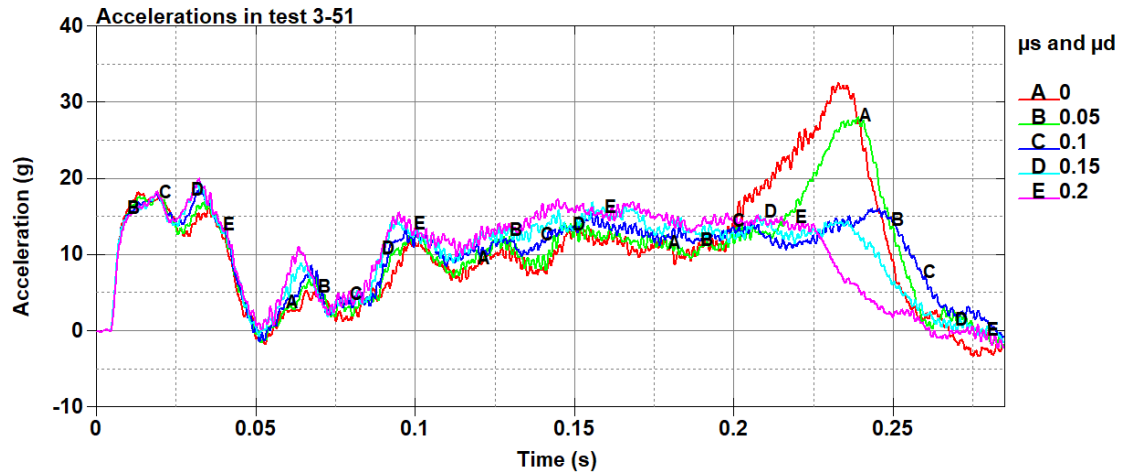


Figure 5.9. Acceleration plots for the pickup truck for different friction coefficients.

Velocity and displacement for test 3-51 are shown in Figures 5.10 and 5.11 respectively. It can be seen from the velocity plots that there is a sharp decline in velocity of the pickup truck for models with friction coefficients 0 and 0.05 when the total stroke length of the tubes is consumed. It can be seen from the displacement plots that the total displacement of the pickup truck is lower as friction increases.

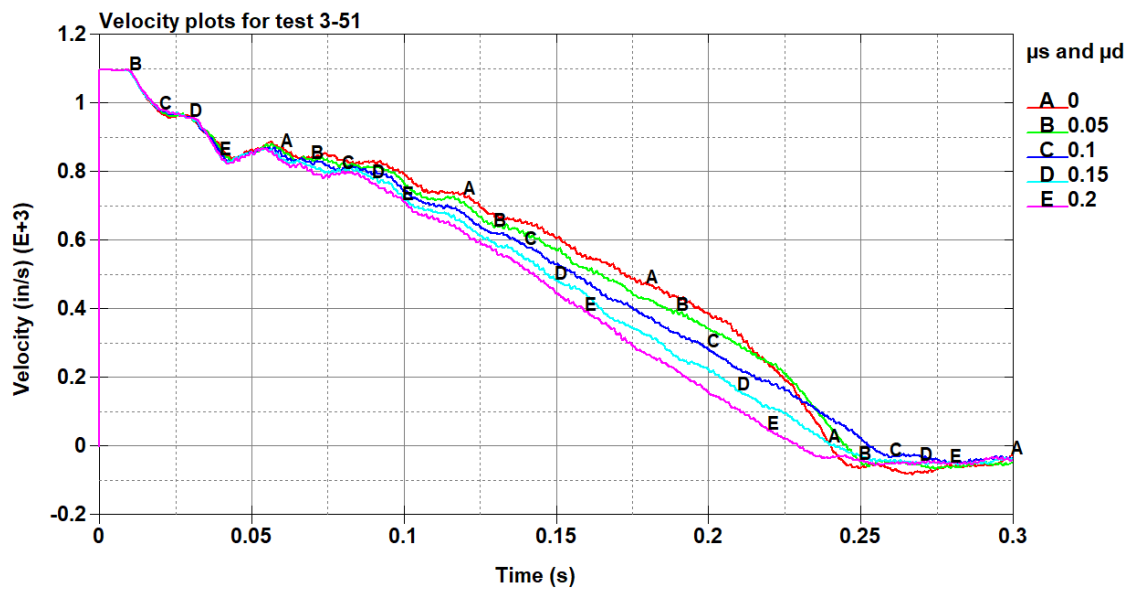


Figure 5.10. Velocity plots of the pickup truck model for different friction coefficients.

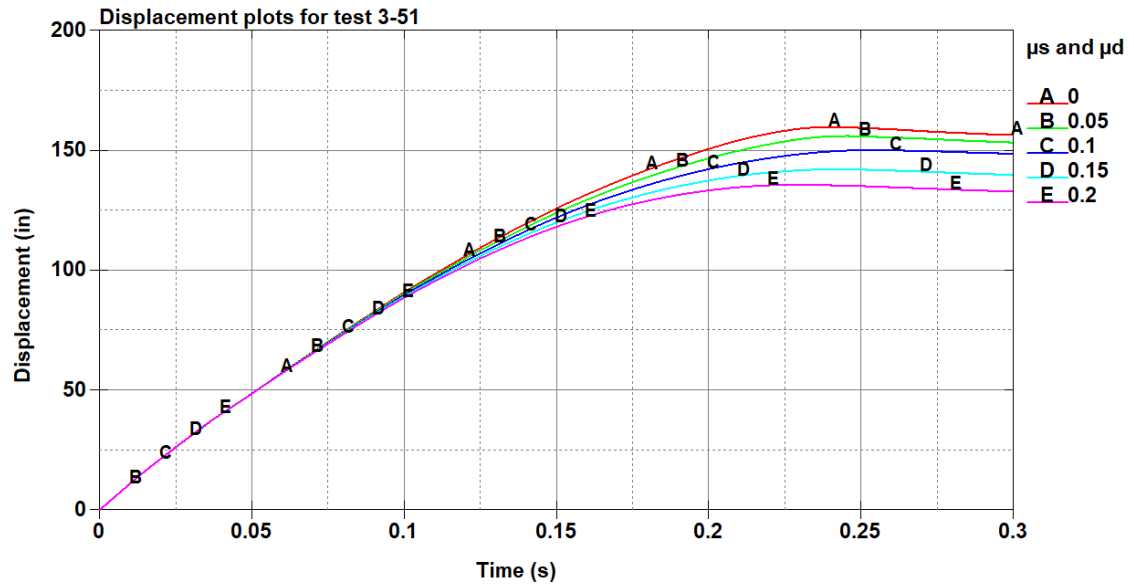


Figure 5.11. Displacement of the pickup truck with time for different friction coefficients.

Kinetic energy of the pickup truck model for varying friction coefficients is shown in Figure 5.12. The kinetic energy plots also show that there is a sharp decline in kinetic energy of the pickup truck for models with lower friction coefficients when the total stroke length of the tubes is consumed. Table 5.2 lists the average force produced by the system for varying friction in the model. The average force increases from 35 kip to 60 kip when the coefficients of static and dynamic friction are varied from 0 to 0.2.

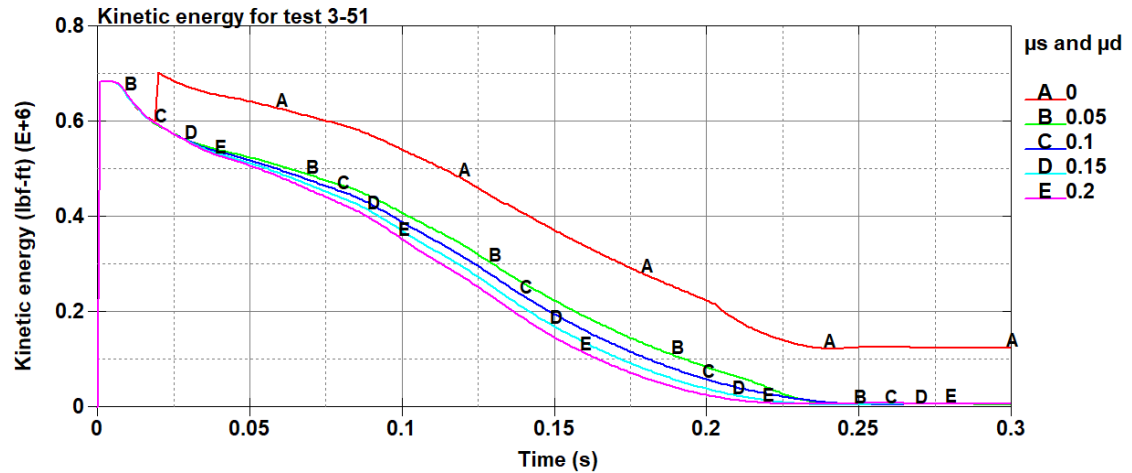


Figure 5.12. Kinetic energy of the pickup truck for different friction coefficients.

Table 5.2. Average forces produced in the model for test 3-51.

μ_s and μ_d	Initial K.E. (lbf-ft)	Final K.E. (lbf-ft)	Δ K.E. (lbf-ft)	Total displacement (ft)	Average force (lbf)
0	6.86e5	2.18e5	4.68e5	13.25	35321
0.05	6.86e5	5.28e4	6.33e5	12.99	48730
0.1	6.86e5	2.41e4	6.62e5	12.47	53087
0.15	6.86e5	5.74e3	6.80e5	11.84	57432
0.2	6.86e5	7.37e3	6.79e5	11.25	60356

The energy balance for test 3-51 is shown in Figure 5.13. The kinetic energy of the system decreases with time and the internal energy increases, balancing the total energy. The hourglass energy in the model is negligible which is desirable. The sliding interface energy increases with time and becomes constant after the pickup truck stops.

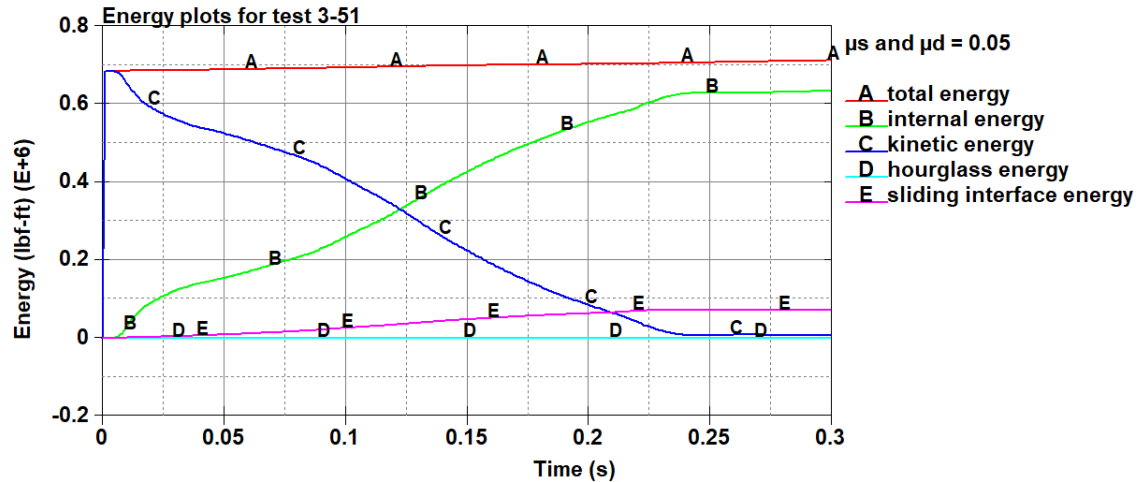


Figure 5.13. Energy balance for test 3-51.

5.3. Occupant Safety Parameters

The 10-ms average longitudinal occupant ride-down accelerations (RAs) and longitudinal occupant impact velocities (OIVs) calculated for tests 3-50, 3-51, 3-52 and 3-53 are listed in Table 5.3. The RA and OIV values for tests 3-50 and 3-51 are within the MASH recommended limits for most coefficients of friction in the model. The values of RA for test 3-52, and both OIV and RA for test 3-53 exceed the recommended values but these can be improved in future studies.

For test 3-50, the OIV exceeds the MASH recommended limits for high coefficients of friction such as 0.2. Such high friction is unlikely to occur in the model but will need to be verified by experimental results. For test 3-51, the RA values exceed the MASH recommended limits for lower coefficients of friction such as 0.05. Although there is some numerical friction present in LS-DYNA modeling, a friction coefficient of 0 is unlikely to occur, so the high RA value for the 0 value of μ_s and μ_d should be acceptable for this research study. The RA value of 28 g's for friction coefficient of 0.05 in test 3-51 occurs

at the end of the stroke and is of a lesser concern because the velocity of the pickup truck is reduced to 20 ft/s (13.69 mph) when it occurs. It has been found in the several models developed in this study that limiting the OIV for test 3-50 and limiting the RA at the end of the stroke length for test 3-51 is critical in development of a working model. The final finite element model described in this study aims to keep the OIV for test 3-50 under limits while also dissipating more energy at the later portion of the stroke to keep the RA for test 3-51 under limits. Since coefficients of static and dynamic friction have been used as parameters for comparative study of the models, experimental verification will be required to determine the exact values in order to optimize the design. However, for test 3-51 where the entire energy of the pickup truck is not dissipated at the end of the stroke length, a second stage energy dissipation mechanism can be developed and incorporated in the docking station if deemed necessary from experimental tests. The possible movement in the support truck will also play a role in lowering the high OIV values in test 3-50 and the high RA values in test 3-51. The lateral occupant ride-down acceleration and lateral occupant impact velocity have lower values in comparison to longitudinal values and are not of concern for this design. Hence, they are not included in the results.

Table 5.3. Occupant risk factors from finite element models for tests 3-50 to 3-53.

Test	Coefficients of static and dynamic friction (μ_s and μ_d)	Occupant impact velocity (OIV), ft/s	10 ms average peak Ride Down Acceleration (RA), g
50	0	37.54	17.9
	0.05	38.19	18.1
	0.10	39.83	17.7
	0.15	40.16	18.8
	0.2	41.80	19.3
51	0	29.67	32.6
	0.05	31.3	28.0
	0.1	32.94	16.1
	0.15	33.93	16.9
	0.2	35.24	17.4
52	0.05	30.97	26.2
	0.1	31.96	26.1
53	0.05	44.75	40.4

CHAPTER 6- CONCLUSIONS AND RECOMMENDATIONS

6.1. Conclusions

This research study serves as an effort to develop the tube folding technology for truck mounted attenuators with the use of computational mechanics. The finite element model developed in this study was optimized to work for most of the test conditions recommended by MASH for evaluation of TMAs. Experimental tests are required for validation of the numerical models, and further development is required to achieve functionality of the design.

Some of the conclusions of this research study are listed below.

- 1) A novel tube folding mechanism for a truck mounted attenuator is designed in this study. The designed mechanism is evaluated using criteria recommended in MASH.
- 2) Numerical models of the designed TMA have been developed using LS-DYNA to simulate impact with passenger vehicles.
- 3) The developed finite element models are subjected to tests 3-50, 3-51, 3-52 and 3-53 recommended by MASH.
- 4) Continuous development of finite element models has been done to optimize the design of the TMA in order to satisfy the criteria of structural adequacy, occupant safety and post-impact vehicular response.

- 5) The designed TMA seems capable of dissipating impact energy of passenger vehicles for tests 3-50 and 3-51 by bringing them to a controlled stop within the occupant safety criteria.
- 6) The designed system has not been optimized for tests 3-52 and 3-53. Further development in the model needs to be done to enable successful functioning of the TMA for these tests.

6.2. Recommendations

The current research study aimed to design and optimize the tube folding technology of a TMA to satisfy the evaluation criteria recommended by MASH. Although satisfactory numerical results have been obtained, the design needs to be validated and further developed through future studies. Some of the recommendations for future research are as follows:

- 1) Full-scale crash testing should be done to validate the numerical models. The design of the TMA should be optimized based on experimental results.
- 2) Models of full-scale crashes including support vehicle, docking station and mounting hardware should be developed.
- 3) Structural changes should be made in the model to ensure proper functioning for tests 3-52 and 3-53.
- 4) A study of the effects of vibrational and fatigue loads on the functions of the designed TMA should be performed.

REFERENCES

- AASHTO. (2009). *Manual for Assessing Safety Hardware*.
- Dean L. Sicking, J. R. (2003). Development of Trailer Attenuating Cushion for Variable Message Signs and Arrow Boards. *Transportation Research Record*, 65-73.
- Giovanni Belingardi, J. O. (2010). Design of the Impact Attenuator for a Formula Student Racing Car: Numerical Simulation of the Impact Crash Test. *Journal of the Serbian Society of Computational Mechanics*, 52-65.
- John F. Carney, D. C. (1999). Reusable High-Molecular-Weight, High-Density Polyethylene Crash Cushions for Wide Hazards. *Transportation Research Record*.
- Livermore Software Technology Corporation. (2019). Retrieved from LSTC:
<https://www.lstc.com/>
- Mitchie, J. D. (n.d.). Collision Risk Assessment Based on Occupant Flail-Space Model. *Transportation Research Record*.
- Murat Buyuk, A. O. (2018). Impact Performance Evaluation of a Crash Cushion Design Using Finite Element Simulation and Full-Scale Crash Testing. *Safety*.
- National Highway Traffic Safety Administration. (2017). *Traffic Safety Facts*.
- Paul Du Bois, C. C. (2004). *Vehicle Crashworthiness and Occupant Protection*. Michigan: American Iron and Steel Institute.

Waszczuk, K. G. (2013). *Development of Efficient Finite Element Model for Truck Mounted Attenuator.*

World Health Organization. (2018). *Global Status Report on Road Safety.*